SKI Report 99:27

Surface Films and Corrosion of Copper

Jouko Hilden
Timo Laitinen
Kari Mäkelä
Timo Saario
Martin Bojinov

March 1999

ISSN 1104-1374
ISRN SKI-R--99/27--SE

SKI

SKI Report 99:27

Surface Films and Corrosion of Copper

Jouko Hilden
Timo Laitinen
Kari Mäkelä
Timo Saario
Martin Bojinov

VTT Manufacturing Technology, Materials and Structural Integrity,
P.O. Box 1704, FIN-02044 Espoo, Finland

March 1999

SKI Project Number 97153

CONTENTS

PREFACE

This report summarises results from several projects carried out as part of a research program funded by Swedish Nuclear Power Inspectorate (SKI) and Radiation and Nuclear Safety Authority, Finland (STUK). Co-operation with Christina Lilja, SKI, and Juhani Hinttala, STUK, is gratefully acknowledged. The reports published earlier are STUK-YTO-TR 105 (1996), “Environmentally assisted cracking behaviour of copper in simulated ground water, STUK-YTO-TR 106 (1996), “Electrical properties of oxide films formed on copper in 0.1 M borax solution”, STUK-YTO-TR 134 (1997), “The effect of chlorides on the electric properties of oxide films on copper” and SKI Report 96:80 (1996), “The effect of nitrite ion on the electric properties of oxide films on copper”.

Espoo, March 10, 1999

Authors

1 SUMMARY

In Sweden and Finland the spent nuclear fuel is planned to be encapsulated in cast iron canisters that have an outer shield made of copper. The copper shield is responsible for the corrosion protection of the canister construction.

General corrosion of the copper is not expected to be the limiting factor in the waste repository environment when estimating the life-time of the canister construction. However, different forms of localised corrosion, i.e. pitting, stress corrosion cracking (SCC), or environmentally assisted creep fracture may cause premature failure of the copper shield. Of the probable constituents in the groundwater, nitrites, chlorides, sulphides and carbonates have been suggested to promote localised corrosion of copper.

The main assumption made in planning this research program is that the surface films forming on copper in the repository environment largely determine the susceptibility of copper to the different forms of localised corrosion. The availability of reactants, which also may become corrosion rate limiting, is investigated in several other research programs. This research program consists of a set of successive projects targeted at characterising the properties of surface films on copper in repository environment containing different detrimental anions. A further aim was to assess the significance of the anion-induced changes in the stability of the oxide films with regard to localised corrosion of copper. This report summarises the results from a series of investigations on properties of surface films forming on copper in water of pH = 8.9 at temperature of T = 80 ^{o}C and pressure of p = 2 MPa.

The main results gained so far in this research program are as follows:

- The surface films forming on copper in the thermodynamic stability region of monovalent copper at 80 ^{o}C consist of a bulk part (about 1 μm thick) which is a good ionic and electronic conductor, and an outer , interfacial layer (0.001…0.005 μm thick) which shows p-type semiconductor properties
- The thin outer layer controls the corrosion properties of copper, corrosion rate being limited by ionic transport through the layer and the charge transfer step of the film dissolution
- Chlorides cause a breakdown of the oxide film in the stability region of divalent copper, but they seem to have no effect on the properties of the film in the stability region of monovalent copper; oxidising conditions with simultaneous exposure to chlorides are thus expected to subject copper to localised corrosion
- Sulphides at the concentration of 10 ppm dissolved H_2S were found not to promote the formation of a three-dimensional film of Cu_2S (or other copper sulphides), thus the mechanisms of localised corrosion which operate under reducing conditions and are based on the formation of copper sulphides seem not to be valid. In the presence of 10 ppm H_2S the corrosion rate of copper is controlled by the charge transfer step of the dissolution of the outer layer.

SAMMANFATTNING

Både i Finland och Sverige har slutförvaringen av använt kärnbränsle tänkt ske genom inkapsling i gjutjärnsbehållare med ett kopparhölje, där kopparhöljet fungerar som kapselns korrosionsbarriär.

Korrosion av kopparhöljet anses inte vara den faktor som begränsar livslängden för kapseln under slutförvarsförhållandena. Olika former av lokala skademekanismer som t.ex. gropfrätning, spänningskorrosion, spänningskorrosion-sprickbildning samt accelererad krypning till följd av omgivningens påverkan kan skada kopparhöljet betydligt fortare än väntat. Vissa element i grundvattnet som t.ex. klorider, sulfider och karbonat har visat på tendenser att främja lokal korrosion av koppar.

Vid planeringen av detta projekt har huvudantagandet gjorts att ytfilmsbildningen på kopparytan bestämmer materialets känslighet för lokala korrosionsattacker under omgivningens påverkan. Projektet ingår i ett forskningsprogram som består av flera på varandra följande projekt som inriktar sig på att påvisa ytfilmens betydelse vid korrosion av kapselns kopparhöje under slutförvarsförhållanden och med förutbestämda koncentrationer av anjoner. Förekomsten och koncentrationen av olika reaktiva element som påverkar korrosionshastigheten undersöks i flera andra forskningsprogram. Denna rapport är ett sammandrag av resultat från en serie ytfilmsmätningar av koppar i vatten vid en temperatur av 80°C (pH 8.9) och ett tryck på 2 MPa.

Huvudresultat hittills i forskningsprogrammet:

- Ytfilmen som bildas på kopparytan vid 80°C består av en 1μm tjock ytfilm som leder både joner och elektroner samt ett semikonduktivt gränsskikt av tjockleken 0.001 - 0.005 μm.
- Det tunna gränsskiktet bestämmer huvudsakligen kopparns korrosionskänslighet, eftersom korrosionshastigheten bestäms av jontransporten genom gränsskiktet och laddningsöverföringssteget vid upplösningen av gränsskiktet.
- Klorider orsakar nedbrytning av CuO-baserade ytfilmer som förekommer under oxiderande förhållanden men påverkar inte Cu_2O-filmen; oxiderande förhållanden med klorider närvarande förväntas därför förorsaka lokal korrosion av koppar.
- Sulfider i en koncentration av 10 ppm (H_2S) visade på bildningen av Cu_2S (eller andra sulfider). Lokal korrosion vid reducerande förhållanden baserad på bildning av kopparsulfider verkar dock inte troligt.

2 INTRODUCTION

In Sweden and Finland the spent nuclear fuel is planned to be encapsulated in cast iron canisters that have an outer shield made of copper. The effect of the repository environment on the life time of the canister and its materials needs to be known when the barrier properties of the canister are estimated.

The copper shield is responsible for the corrosion protection of the current canister construction. General corrosion of the canister shield is currently estimated not to be the life-limiting factor in the waste repository environment. However, different forms of localised corrosion, i.e. pitting corrosion, environmentally enhanced creep fracture and stress corrosion cracking (SCC) phenomena, may potentially limit the protective properties of the copper canister.

The repository environment is oxidising for some time after closing up, but is considered to become reducing when oxygen is consumed, and to stay reducing unless replenishment of oxygen occurs e.g. during an ice age. However, the oxides that form on copper during the manufacture are typical for an oxidising environment, and reduction of these oxides can be very slow. Therefore, information on the susceptibility of copper to localised corrosion after exposure to both oxidising and reducing environments is needed.

This project is a part of a larger long term research program called “Correlation of Oxide Film Properties and Susceptibility to Localised Corrosion in Repository Environment”. The program was launched in order to develop a mechanistic understanding as well as a sufficient database for assessing the possibility of stress corrosion cracking and the extent of pitting of copper under the expected disposal vault conditions. The main assumption made in planning this research program is that the surface films forming on copper in the repository environment largely determine the susceptibility of copper to the different forms of localised corrosion. A proper characterisation of surface films forming on copper in repository environment is not available, and thus a considerable part of this research program is devoted to such a characterisation. New surface sensitive techniques have become available, which pinpoints the need for a more detailed investigation of the role of the surface films. As this type of approach is rather new, experimental work needs to be performed not only in simulated ground water but also in solutions with more accurately controlled properties. Borate solutions are used in order to establish a constant pH.

Each project of the program consists of characterisation of the electrochemical and electrical properties of the surface films on copper in a given environment. The projects are shown in Table I. The surface film characterisation work is supported by separate projects in which modelling of pitting and stress corrosion cracking of copper is being performed.

In general, the corrosion rate of any metal increases exponentially with temperature. This assumes that there is a fast supply of oxidant and no accumulation of inhibiting corrosion products such as a persisting layer. In the repository conditions at the depth of 500 metres the hydrostatic pressure alone can be 5 MPa. Mor et al. studied effects of temperature on the corrosion in sea water at different hydrostatic pressures and

concluded that copper corrosion rate is always increased by a pressure rise and that the increased corrosion rate is further accelerated by increasing temperature [1]. The increase in hydrostatic pressure can accelerate cathodic or anodic processes depending on the conditions. In order to guarantee relevant experimental conditions, the tests of all the projects were carried out under elevated pressure in an autoclave.

Table I. List of projects. TBS = tetraborate solution (0.1 M $Na_2B_4O_7$, T = 80 ^oC, p = 2 MPa), RGW = Reference Ground Water.

Environment	Redox-conditions	Year of completion
TBS	Reducing	1996
TBS + $NaNO_2$	Oxidising	1996
TBS + Cl^-	Reducing	1997
TBS + S^{2-}	Reducing	1998
TBS + CO_3^{2-}	Reducing	1999
RGW + anions	Reducing	1999

This report gives an overview on the main results from tests performed in pure tetraborate solution and in tetraborate solution with chlorides. The results from tests performed in tetraborate solution with nitrites showed that nitrites do not have a noticeable effect on the surface film properties. Thus these tests are not reviewed in this report.

In addition to the overview of earlier results, a detailed description of test results on the effect of sulphide ions in the form of 10 ppm dissolved H_2S is reported. The purpose of the new experimental work described in this report was to characterise the electrical and electrochemical properties of surface films forming on copper in tetraborate solution with 10 ppm of S^{2-} covering the fourth environment shown in Table I.

3 LITERATURE SURVEY ON CORROSION OF COPPER IN SULPHIDE SOLUTIONS

3.1 Introduction

Many literature reviews on the corrosion of copper have been presented [2-5]. However, little information can be found about the behaviour of copper in sulphide solutions. Sequeira [6] presents some potential-pH diagrams for the Cu-S-H_2O system, but does not give any references to experimental corrosion studies of copper in solutions containing sulphide ions. Some natural analogue studies have been made to model the corrosion of copper in repository conditions containing sulphide species [7,8].

It has been proposed that corrosion of copper is controlled by the availability of dissolved sulphide ions in the groundwater passing onto the surface of the canister i.e. the diffusivity of sulphide in the bentonite clay, inside of which the canister is placed [9,10]. If this is the only source of sulphide, then the life time of the canister would be over 10^6 years even if rather conservative pitting factors are assumed [11]. However, according to the present knowledge the role of sulphate ions as a source of additional sulphide can not be excluded. It has been shown that the kinetic inhibition of the direct oxidation of copper by sulphate is so strong that no examples of this kind of inorganic reduction at repository relevant temperatures are known [12]. But sulphate ions may act as a source for sulphide ions if they are reduced by micro-organisms, as described below.

The role of sulphate as a source for sulphide has been debated ever since the existence of the sulphate reducing bacteria (SRB) under hostile repository conditions was suggested in the beginning of 1980's. These micro-organisms can reduce sulphate to sulphide according to the following schematic reaction:

$$SO_4^{2-} + 4H_2 \rightarrow S^{2-} + 4H_2O \quad (1)$$

In reports published in the of 1980's and early 1990's it was assumed that bacterially assisted sulphate reduction is possible, but it was suggested to be limited by the availability of organic matter in the repository and the groundwater [9,13]. This seems to include the assumption that the only possible micro-organisms able to reduce sulphate would be heterotrophs, i.e. micro-organisms which use organic matter as a carbon source. In later reports the existence of autotrophs, i.e. micro-organisms which can use dissolved CO_2 has also been discussed [14]. AECL Research studied the effects of sulphide produced by SRB, but with the assumption that the biofilm is not present on the canister surface [15], because of the radiation and heat effects were supposed to restrict the populations close to the containers. Sulphide ion concentrations as high as 10^{-2} M have been shown to be possible by SRB within biofilms [16], but reliable estimates for the concentrations outside the biofilm are difficult to give.

If it is true that significant amounts of sulphate can be reduced to sulphide by SRB, then also kinetic and pitting aspects of sulphide-assisted corrosion of copper become more important. As an example, in their scooping calculations Worgan et al. modelled also a situation where sulphate is reduced to sulphide by sulphate reducing bacteria (SRB) and

a pitting factor of 5 was adopted. Time to failure by pitting corrosion in their case was estimated to be about 10000 years [11].

This shows that the possible risks for sulphide-induced localised corrosion of copper should not be neglected. To address this question and to plan the experimental part of this work, a short literature survey on different aspects of the influence of sulphide ions on the behaviour of copper was made. This survey comprises a description of the thermodynamic stability of the oxidation products and of the composition of the surface films on copper in the presence of sulphide ions, results on the effect of sulphide ions on the voltammetric behaviour of copper and comments on the influence of sulphide ions on the corrosion (especially pitting corrosion) of copper.

3.2. Thermodynamic stability of copper and its oxidation products

Copper is considered a semi-noble metal having an intermediate thermodynamic stability. It is normally stable in non-aerated acid or neutral media, but can corrode in the presence of oxygen. Contrary to these assumptions, Hultquist measured copper to be oxidised by water with hydrogen evolution [17], but later studies by other researchers seem to show that his results were erroneous due to inadequately controlled experimental conditions [18,19].

The presence of sulphide ions makes possible the formation of copper sulphides in the surface film on copper. The equilibrium potentials (given vs. NHE) at 25°C for the electrochemical formation of Cu_2S and CuS are

$$2\,Cu(s) + S^{2-}(aq) \leftrightarrow Cu_2S(s) + 2e^- \quad E_1/V = -0.890 + 0.0295\ p[S^{2-}] \qquad (2)$$

$$Cu(s) + S^{2-}(aq) \leftrightarrow CuS(s) + 2e^- \quad E_2/V = -0.698 + 0.0295\ p[S^{2-}] \qquad (3)$$

For the latter potential the temperature dependence is $\partial E_2 / \partial T = -1.040$ mV/°C.

The following pH dependent ionic equilibria determine the predominant sulphide species

$$H_2S \leftrightarrow HS^- + H^+ \quad pK_4 = 7.04 \qquad (4)$$

$$HS^- \leftrightarrow S^{2-} + H^+ \quad pK_4 = 11.96 \qquad (5)$$

Although copper is not oxidised in water with low oxygen content in the absence of sulphide ions, the values of the equilibrium potentials given above show that copper may be oxidised even in the absence of oxygen when HS^- is present. As a result, copper and copper alloys are normally not selected for environments known to contain high concentrations of sulphur or sulphides.

The thermodynamic stability of metals can be illustrated by means of potential-pH (Pourbaix) diagrams. These have been also widely used to predict corrosion of copper. The potential-pH diagram indicates the conditions for immunity, passivation and corrosion. It does not, however, give any information about the rate of the possible corrosion reactions, or the effectiveness of passivation.

3.2.1. Potential-pH diagrams for bulk oxidation products in the presence of sulphide ions

Potential-pH diagrams for the system Cu-S-H_2O are available from several sources [6, 20, 21]. Some potential-pH diagrams have been calculated specially when studying the repository of nuclear waste [22, 23]. In these diagrams non-stoichiometric sulphide minerals djurleite $Cu_{1.934}S$ and anilite $Cu_{1.75}S$ are also taken into account, not only chalcocite (cuprous sulphide) Cu_2S and covellite (cupric sulphide) CuS. In the latter of these studies a literature review of earlier thermodynamic calculations is presented. Other collections of references to thermodynamic studies has been supplied by Sequeira [6].

Figures 1a, 1b, 2a and 2b show some potential-pH diagrams from the literature. In Figures 1a and 1b the stability fields of different copper sulphides are shown while in Figures 2a and 2b the formation of different copper oxides has been taken into account.

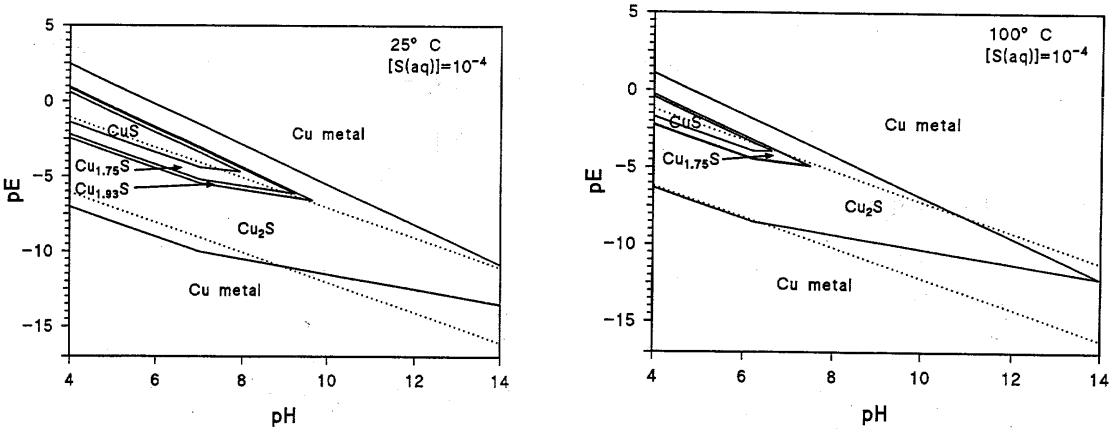

(a) (b)

Figure 1. Stability fields of metallic copper and different copper sulphides at temperatures 25°C and 100°C, activity of dissolved sulphur $[S] = 10^{-4}$ *(either as* HS^- *or* SO_4^{2-}*). Dotted lines indicate the pE-range at which water can act as oxidant, upper limit* $[H_2] = 10^{-9}$ *corresponds to the estimated lowest concentration of* $H_2(aq)$*, lower limit corresponds to the* $H_2(aq)$ *activity of 1* [23]. *The variable pE is defined as* $pE = \frac{nF}{2.303RT}E$, *where E is potential and n is the number of electrons.*

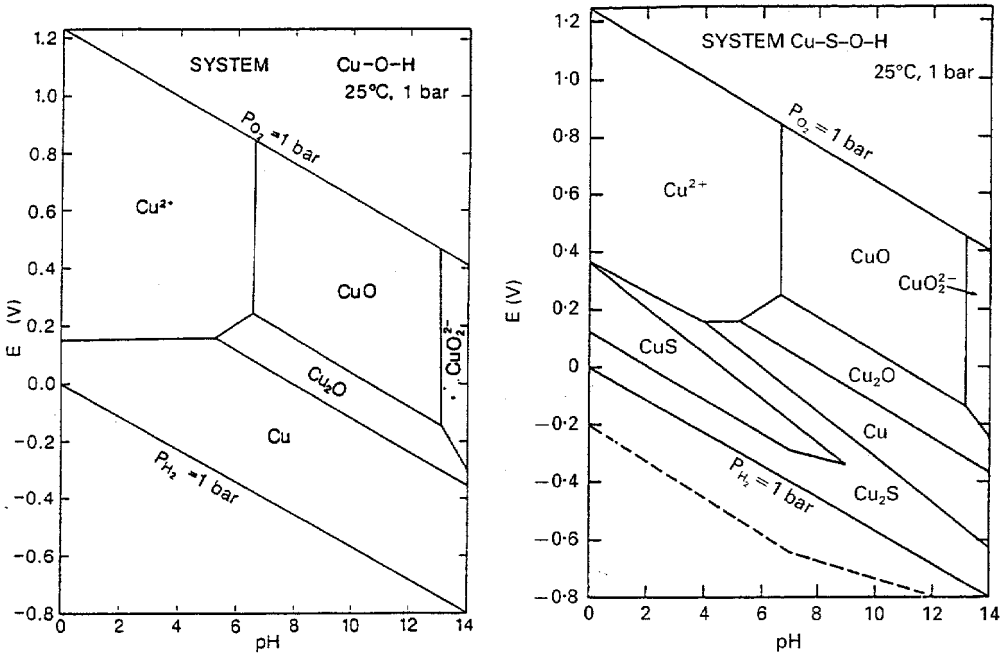

(a) (b)

Figure 2. (a) Potential-pH diagram for part of the Cu-O-H system: assumed activity for dissolved Cu=10^{-6}; potentials relative to NHE; (b) Potential-pH diagram for part of the Cu-S-O-H system: assumed activity for dissolved Cu=10^{-6}; potentials relative to NHE.

The diagrams demonstrate the possibility of the formation of copper sulphides at potentials well below the equilibrium potential for the Cu(I)/Cu couple in the absence of sulphide ions.

Experimental checks of the potential-pH diagrams of copper-sulphur-water systems have not been published since the very early study of Horvath [24].

3.2.2. Potential-pH diagrams of bidimensional layers of adsorbed elements on metal surfaces

The potential-pH diagrams discussed in the preceding chapter have been constructed by using thermodynamic values of bulk substances. However, when an aggressive anion, such as sulphide is adsorbed on the metal surface, surface energies should also be taken into account. Due to high surface energies, adsorbed layers may be formed in potential - pH domains where a classical diagram does not predict such phases. This phenomenon must not be neglected, because an adsorbed monolayer or even part of such layer can induce marked changes in the reactivity of the metal.

Marcus has extended the principle of potential-pH diagrams to the case of bi-dimensional layers of adsorbed elements on metal surfaces [25]. He and his co-workers have calculated potential-pH diagrams for sulphur adsorption on surfaces of iron, nickel and chromium [26]. Their calculations show that adsorbed sulphur layers can be present under conditions in which bulk sulphide is not stable. The source of the sulphur can be sulphur inclusions of the metal or dissolved sulphur species (S, H_2S, HS^-, $S_2O_3^{2-}$, HSO_4^-

and SO_4^{2-}) from water. In their calculation Marcus et al. noticed that detrimental effects of sulphur extend to the range where sulphides are not thermodynamically stable.

3.3. Composition of corrosion layer on copper in the presence of sulphide ions

The composition of the sulphide layer formed may have a great influence on the corrosion resistance of copper. For example djurlite, unlike other sulphides, has been reported to provide corrosion protection [15]. The composition of the copper sulphide layer has been determined in several investigations, but the results seem not to be applicable to the disposal vault conditions, because the composition of the layer has a strong dependence on its history [27-32].

For example, de Chialvo et al. [27] suggest that the copper sulphide in an alkaline solution changes its structure as follows, when the potential is increased in the positive direction:

$$Cu \rightarrow Cu / Cu_{1.8}S \rightarrow Cu / Cu_{1.8}S / Cu_2S \rightarrow Cu / Cu_{1.8}S / Cu_2S / CuS \qquad (6)$$

They proposed the following reactions for the initiation of the growth of the sulphide layer:

$$2\,Cu(s) + S^{2-}(aq) \leftrightarrow Cu(HS)_{ad} + 2e^- \qquad (7)$$

or

$$2\,Cu + S^{2-} \leftrightarrow Cu_2S + 2e^- \qquad (8)$$

Khairy et al. concluded that the film which is formed consists of a $Cu/Cu_{2-\delta}S$ layer which is over-layered with CuS [28, 29]. Scharifker et al. [31] concluded that the film formed on copper surface in their voltammetric experiments has the stoichiometry of Cu_2S with chalcocite structure.

3.4. Voltammetric studies

Voltammetric measurements are a tool to obtain an overview of the electrochemical behaviour of a material at different potentials and to obtain preliminary kinetic information. Unfortunately, all the studies found in the literature concerning copper-sulphide systems at moderately alkaline solutions have been performed using carbonate-based buffer solutions [27, 31]. These results cannot be directly applied to nuclear waste repository conditions, because the literature data indicates that voltammetric behaviour of copper may be greatly influenced by the composition of the electrolyte solution. This is illustrated in Figures 3a and 3b, in which voltammograms of copper in moderately alkaline solutions of different composition are presented. Differences between the voltammograms are considerable, although the pH values of the solutions are quite close to each other.

In the voltammogram of copper in a borate buffer solution (Fig. 3a), peaks AI and CI have been ascribed to the formation and reduction of the Cu(I) oxide, i.e. Cu_2O, respectively [33]. Peaks AII and CII refer to formation of CuO_2^{2-} and $CuO/Cu(OH)_2$, and

reduction of $CuO/Cu(OH)_2$, respectively. On the other hand, the voltammogram in a mixture of carbonate and bicarbonate is more complicated (Fig. 3b). It is possible that the formation of copper carbonate species (malachite $CuCO_3Cu(OH)_2$) can take place at such a high concentration of carbonate species at pH 9.8 [5]. It is important to note that the differences may also to a considerable extent be due to the different potential sweep rates.

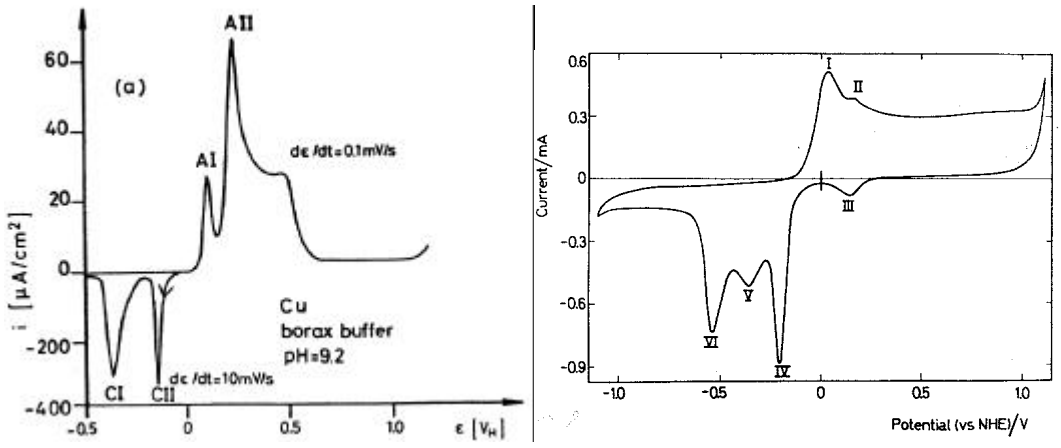

Figure 3. (a) Copper electrode in borax buffer , pH = 9.2, potential sweep rate 0.1mVs^{-1} [33]; (b) Copper in 0.1 M $NaHCO_3$ + 0.1 M Na_2CO_3 pH 9.80, potential sweep rate 200mVs^{-1}. Apparent copper electrode area 0.322cm^2 [27].

Because of the different experimental environment from that in the nuclear waste repository conditions, the discussion below has to be considered with some caution. However, the results reviewed below deserve to be presented in order to give an idea of the possible influences of sulphide ions on the voltammetric behaviour of copper.

The voltammograms of copper measured by De Chialvo et al. [27] in carbonate-based solutions containing sulphide ions (Fig. 4, compare also with Fig. 3b) demonstrate that the presence of sulphide ions leads to the appearance of additional peaks (VII, IX and X) and changes the structure of current peaks. De Chialvo et al. interpreted peak VII to correspond to the formation of copper sulphide, which is formed at potentials close to the equilibrium potentials of the Cu_2S/Cu and CuS/Cu couples. The cathodic peaks observed during the negative-going potential scan suggest that two different copper sulphide may be formed. Their voltammetric results show that formation of the copper sulphide film shifts the threshold potential for the copper oxide formation in the positive direction and increases the cathodic and anodic currents for the film reduction and formation processes.

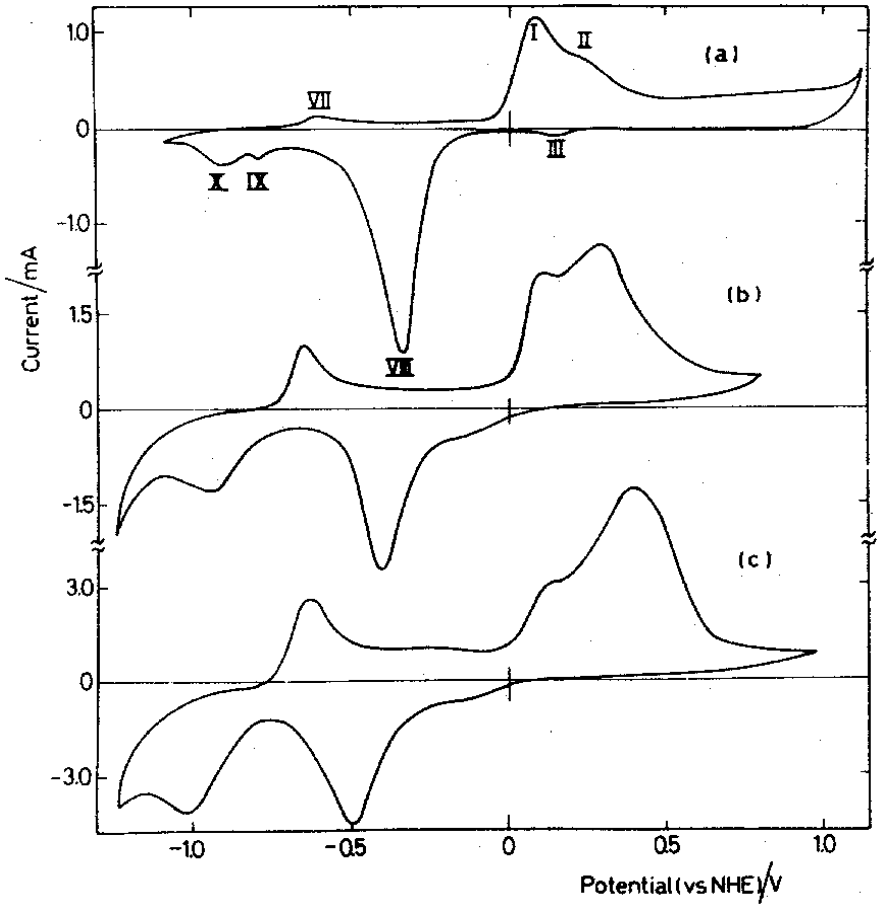

*Figure 4. Voltammograms run with copper electrodes in 0.1 M $NaHCO_3$ + 0.1 M Na_2CO_3 + x Na_2S at 200mVs^{-1}. a) x = 10^{-3} M ; b) x = 5*10^{-3} M ; c) x = 10^{-2} M. Apparent copper electrode area 0.322 cm^2 [27].*

De Chialvo et al. [27] also found out that the dissolution current at pH 9 increases linearly with the concentration of sulphide in the solution in the potential range where a copper sulphide can be formed (-0.7 V_{NHE} < E < -0.2 V_{NHE}). However, the linear dependence they achieved is difficult to apply to very low concentrations (under 0.001M), because the correlation of the linear regression was not sufficient. When a rotating disc electrode was employed, they noticed that at lower rotation rates the dissolution rate was increased, but no current maximum in the potential range (-0.7 V_{NHE} < E < -0.2 V_{NHE}) was observed. At high rotation rates they observed a current maximum at -0.3 V_{NHE} < E < -0.4 V_{NHE}.

De Chialvo et al. did not detect soluble products during the reactions of copper in a carbonate-based solution of pH 9 containing sulphide ions by means of a rotating copper disc-gold ring electrode. This observation is supported by the results of Scharifker et al., who measured the ratio of Q_a/Q_c (anodic/cathodic charge) in the cyclic voltammogram when potential was swept in the range where copper sulphide is formed [31]. The measured ratio was 1 and independent of pH and of sulphide concentration, which strongly suggests that no soluble products were formed. Another supporting result to the idea that the oxidation and reduction of copper in the presence of sulphide ions are solid

state processes was given by Syrett [32]. He found out that the corrosion rate of copper was not markedly dependent on testing time or hydrodynamic conditions in water with low oxygen content and containing sulphide ions.

It can be concluded that despite the great importance of sulphides in copper corrosion, only few electrochemical and corrosion studies [27-32] have been performed on this matter. Unfortunately, in most of them the sulphide concentration has been much too high to be comparable with repository conditions. Some experimental studies have been published, which were performed in simulated nuclear waste repository conditions [34], but it seems that more experimental studies are needed in relevant conditions. Not only the effect of sulphide ions, but also possible synergetic effects of sulphide with other aggressive ions should be clarified, because the joint actions of different ions are theoretically extremely difficult to model.

3.5 Sulphur-assisted corrosion mechanisms

It has been generally assumed that for copper containers uniform corrosion and possibly pitting will occur during the initial oxidising period. Pitting is the usual form of corrosive attack at surfaces, which have nonprotective films and/or scale deposits or other foreign substances. Growth of a corrosion pit involves a type of anodic reaction, which is an autocatalytic process. In such a process the corrosion within a pit produces conditions which are both stimulating and necessary for the continuing activity of the pit [35].

As reducing conditions are obtained in the disposal vaults, the slow uniform corrosion will be the dominant form of corrosion [36,37,9]. However, studies performed by Vasquez Moll et al. showed that also sulphide induced pitting corrosion of copper may take place in reducing conditions [30]. They found out that the most severe potential for the sulphide influenced pitting corrosion of copper lies just below the threshold potential of copper oxide formation i.e. at -0.1 to -0.2 V_{SHE}. Thierry et al. reported that the production of hydrogen sulphide by sulphate-reducing bacteria might lead to pitting corrosion of copper and copper alloys. In this case corrosion is due to the formation of a thick non-adherent layer of chalcocite (Cu_2S) or covellite (CuS_{1+x}) [38]. Some other results show also that if pitting corrosion occurs in reducing conditions the mechanism involves sulphides [23,39]. However, it should be noticed that results from this kind of voltammetric studies should not be taken as the only basis for conclusions. The environmental history of the surface film, especially cyclic redox conditions, has a great influence on the formation of pits [38,40,41].

Even though there is no clear picture of the mechanism which could explain sulphide induced pitting corrosion of copper, some general aspects of sulphur assisted corrosion mechanisms of different metals summarised by Marcus can be used to clarify the possible role of sulphide ions [25]. According to him, sulphur may accelerate active dissolution of metals, because adsorbed sulphur weakens metal-metal bonds and thus lowers the activation energy for dissolution. This effect can be strongly localised. Sulphur can also poison the passivation process by blocking the sites of adsorption of the hydroxyl ions, which are necessary precursors in the formation of the passive state. The critical value of

sulphur coverage on the surface is 0.7-0.8 monolayers of sulphur atoms. Furthermore the adsorbed sulphur inhibits nucleation of the oxide or diminishes the density of nucleation sites and slows down the lateral growth of the oxide film. When a passive film grows on top of the adsorbed sulphur layer the structure and the properties of the passive film are modified. Current density in the passive state can be several times higher for a film formed with sulphur present at the metal-oxide interface. On the other hand it has been reported that djurlite, unlike other sulphides improves the corrosion resistance of copper [15].

One has to remember that the effects of the various anions in combination might be quite different from those obtained for each anion individually. Synergetic effects can appear and the aggressiveness of one species can be modified by the presence of another species, which can have an accelerating or inhibiting influence. Especially when considering the role of different anions in copper pitting, there exists a large discrepancy concerning the joint action of different anions and even actions of individual anions when the time scale and conditions are changed [42-44]. It seems that more experiments in carefully controlled environments are required to reconcile the theory of pitting corrosion of copper and practical observations in sulfur/suphide containing solutions.

3.6. Electrical properties of surface films on copper in the presence of sulphide ions

In order to correlate the observations concerning the influence of sulphide ions on the corrosion behaviour of copper with measurable quantities, one approach is to characterise the effect of sulphide ions on the electrical properties of the surface films on copper. Schmuki and Boehni have studied pitting corrosion and semiconductive properties of passive films on stainless steels and concluded that there is a correlation between the distribution of localised states in the passive film, i.e., its defect structure, and the stability of the film [45]. It is, however, uncertain whether their results can be used when copper-sulphide films are studied, because possible pitting of copper sulphide film is entirely different from the pitting of passive oxide films on stainless steels.

Khairy et al. studied the conductivity of the sulphide film formed on copper electrodes [28,29]. Calculated values of the specific conductance of the deposited sulphide film were about $3.8*10^{-5}\Omega^{-1}cm^{-1}$. They concluded that the conductivity is due to the defects in the Cu_2S lattice caused by vacant cation sites as well as some Cu^{2+} ions replacing Cu^{+} ions.

4 SUMMARY OF RESULTS IN NEARLY NEUTRAL TETRABORATE SOLUTION

4.1 Introduction

The structure of the passive film on copper in a tetraborate solution has been interpreted to consist of a Cu_2O layer in the stability region of monovalent copper species. At higher potentials the duplex film structure has been interpreted to consist of an inner Cu_2O layer and of an outer $CuO/Cu(OH)_2$ layer [46]. Additionally, substoichiometric CuO_x or adsorbed $Cu(OH)_{ad}$ layers have been empirically detected at low overpotentials [47]. Also higher valence copper oxides $CuO_y \bullet zH_2O$ or copper III oxide have been suggested to exist at high positive overpotentials [48]. Both the film formed in the stability region of monovalent copper (consisting of mainly Cu_2O) and the film formed in the region of divalent copper (consisting of mainly $Cu_2O + CuO/Cu(OH)_2$) have been found to show p-type semiconductive properties [49-57].

4.2 Experimental

Oxygen free phosphorus microalloyed copper (Cu OFP) containing 99.992 wt-% Cu and 45 ppm P produced by Outokumpu Poricopper Oy was used as the test material in all the experiments. The chemical composition of the test material is shown in Table II. The specimens were taken from a sheet hot rolled at temperature from 850°C to 800°C. The properties of the copper sheet analysed by Outokumpu Poricopper Oy are presented in Table III.

Table II*. Composition of the investigated Cu OFP material.*

O / ppm	P / ppm	Fe / ppm	Cu / %
1.5	45	2	99.992

Table III*. Properties of the investigated Cu OFP material.*

tensile strength (MPa)	yield strength (MPa)	fracture strain (%)	grain size (mm)	conductivity (% IACS)
215	52	50	0.09 - 0.12	97.5

Tests were performed in an autoclave in 0.1 M $Na_2B_4O_7$ (tetraborate) solution at 80 °C. The volume of the autoclave was 8 dm^3. Tetraborate solution was made of pro analysis $Na_2B_4O_7$ (Merck 1.06306) and of water prepared in a MILLI-RO® 15 water purification system (Millipore). The pH at 80 °C was estimated to be 8.9 using thermodynamic calculations. Dissolved oxygen was removed from the electrolyte solution by bubbling with a gas mixture of Ar + 3% H_2, after which the autoclave was pressurised to 2 MPa

using the same gas mixture. Electrode surfaces were ground using 4000 grit SiC emery paper.

Potentials were measured against a hydrogen electrode in the same solution. All the potentials in this work are reported versus reversible hydrogen electrode scale (RHE). The potential scale can be changed into the standard hydrogen scale (SHE) by subtracting 0.623 V from the RHE value, i.e. $E_{SHE} = E_{RHE} - 0.623$ V.

Voltammetric measurements were carried out using a Wenking LB 81M potentiostat and a Hi-Tek Instruments PPR1 waveform generator. Impedance measurements were performed by a Solartron ECI 1287/FRA 1260 system in a frequency range 0.01 Hz - 10 kHz at an AC amplitude of 10 mV (rms). Capacitance vs. potential curves were registered at a sweep rate of 1 mVs^{-1}, and a frequency of 540 Hz at an AC amplitude of 10 mV (rms). The electrical properties of surface films were measured using the contact electric resistance (CER) technique. The used CER apparatus was manufactured by Cormet Ltd. Before starting CER tests, air borne oxides were removed from the contact surfaces (diameter 2 mm) using 4000 grit SiC emery paper. The surfaces were rinsed with MILLI-RO® 15 water and pressed together after which the CER apparatus was installed immediately into an autoclave. The contact displacement used was 2 μm which corresponds to a nominal contact pressure (compressive stress) of 0.67 MPa.

4.3. Results and discussion

4.3.1 Voltammetric measurements

Figure 5 shows a potentiodynamic polarisation curve measured with a sweep rate of 0.1 mV/s. In the positive going sweep two anodic peaks (A_I and A_{II}) are seen, indicating the oxidation of metallic copper to monovalent copper, (A_I), and further to divalent copper (A_{II}).

During the negative going sweep the reduction peaks C_{II} and C_I are the reduction counterparts of the oxidation peaks A_{II} and A_I, correspondingly. The peak C_I is split in two parts. A noteworthy feature in the positive going sweep is that the current density in the stability areas of both monovalent copper and divalent copper does not increase as a function of potential. This indicates that the rate limiting step of the oxidation reaction is not a charge transfer step.

The surface film thickness after potentiostatic oxidation for different times was calculated from the charge consumed in cathodic reduction of the films. The results for three different oxidation potentials are shown in Fig. 6. The thickness is in the range of 10^{-6} m. It is noteworthy that the thickness increases clearly more rapidly at the oxidation potential of 0.75 V_{RHE} and at 1.0 V_{RHE} than at 0.6 V_{RHE}.

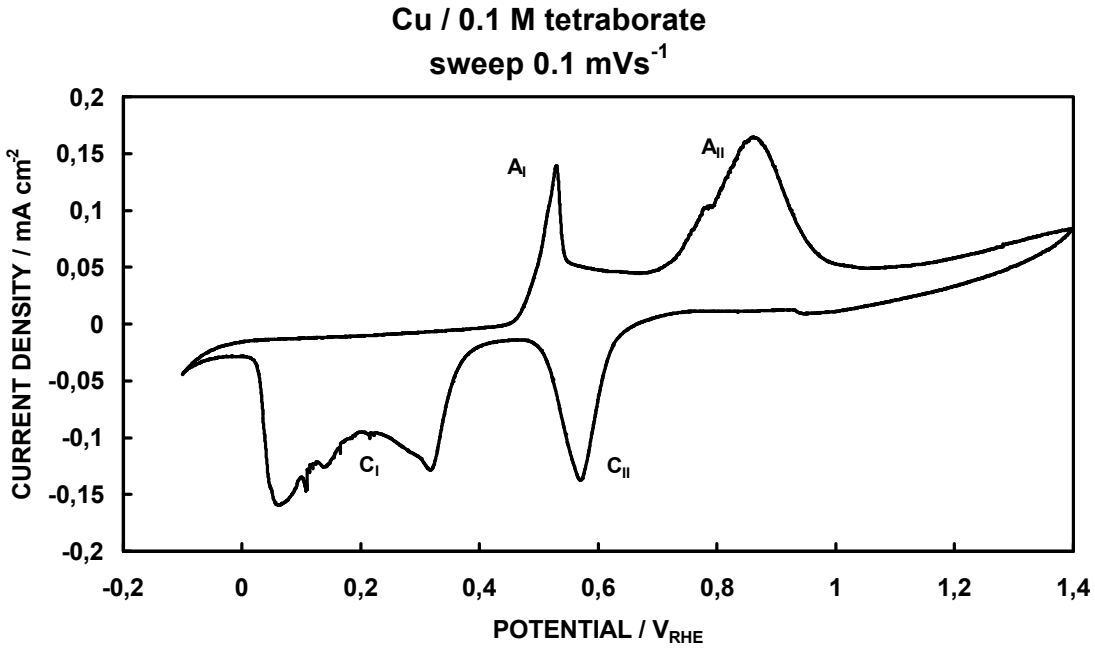

Figure 5. Potentiodynamic polarisation curve of Cu OFP in 0.1 M $Na_2B_4O_7$, T = 80 °C, p = 2 Mpa, sweep rate 0.1 mV/s.

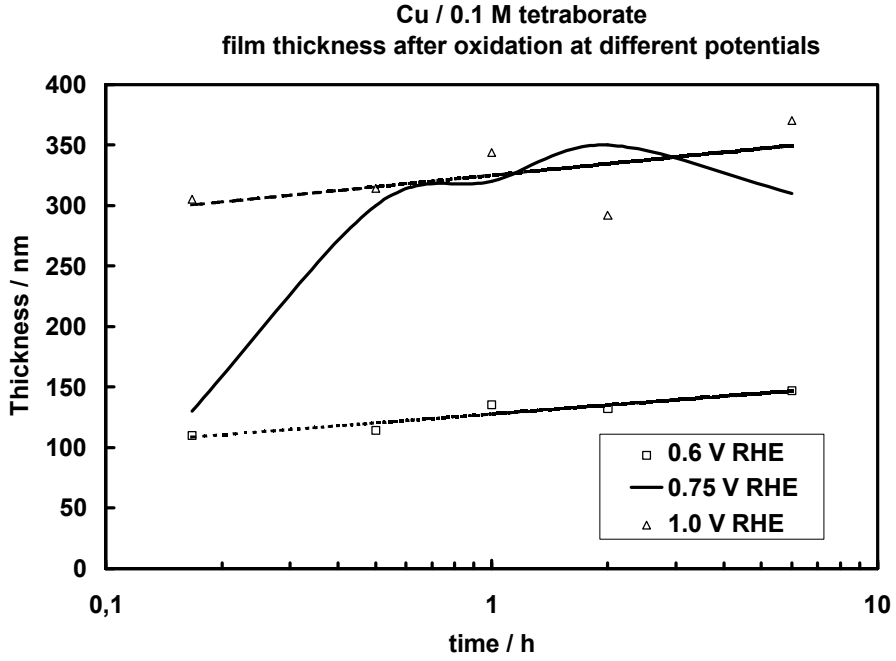

Figure 6. Surface film thickness as a function of oxidation time for Cu OFP in 0.1 M $Na_2B_4O_7$. Data is shown for oxidation potentials of 0.6 V_{RHE}, 0.75 V_{RHE} and 1.0 V_{RHE}.

4.3.2 Resistance-potential curves

The contact electric resistance of the surface film measured in 0.1 M tetraborate solution is shown in Fig. 7 as a function of potential, together with the current density of the CER tips measured simultaneously. The used sweep rate was 0.1 mV/s. The polarisation current of the CER tips shows basically the same features as the one measured with a separate flag type working electrode shown in Fig. 5. Within the potential ranges corresponding to the stability regions of monovalent and divalent copper oxides the current density does not increase as a function of potential. Further, with this slower sweep rate the nearly steady state current density in the potential region of the monovalent copper is equal or slightly higher than that of the divalent copper.

Contact electric resistance is seen to increase by about seven decades at the potential where metallic copper oxidises to monovalent copper, indicating the formation of a surface film containing most probably Cu_2O. The resistance reaches a maximum of about 15 Ωcm^2 and then decreases as the potential increases, which is an indication of p-type semiconductor properties of the oxide. The fine structure of the R vs. E curve (i.e. peaks in resistance situated at about +0.85 V and +1.0 V) are related to the formation of copper (II) compounds, i.e. CuO and $Cu(OH)_2$. Further increase of potential is seen to result in a decrease in resistance.

In the negative going sweep the resistance first increases but then exhibits a minimum at ca. 0.6 V. This minimum coincides with the start of the cathodic current C_{II} due to the reduction of Cu(II) to Cu(I). A subsequent maximum is observed at ca. 0.4 V, after which the resistance decreases to the level of a clean surface at about the same potential at which the reduction current C_I starts to increase. The low value of the resistance indicates that the surface film on copper is reduced totally and also that the film is relatively easy to reduce, as the potential difference between the peak potentials of film formation and reduction is only about 0.2 V. At the potential where monovalent copper oxidises to divalent copper (above 0.7 V) the resistance shows an increase by roughly one order of magnitude. At still higher potentials the resistance decreases when potential increases.

The surface film resistance of Cu OFP in a 0.01 M tetraborate solution (see Fig. 8) was found to be rather similar to that measured in a 0.1 M solution. The first maximum in the value of resistance at about +0.5 V_{RHE} is again related to the formation of the monovalent copper, i.e. Cu_2O. The following maximum in the value of resistance at about +0.8 V_{RHE} and the subsequent plateau are related to the formation of divalent copper compounds such as CuO and $Cu(OH)_2$.

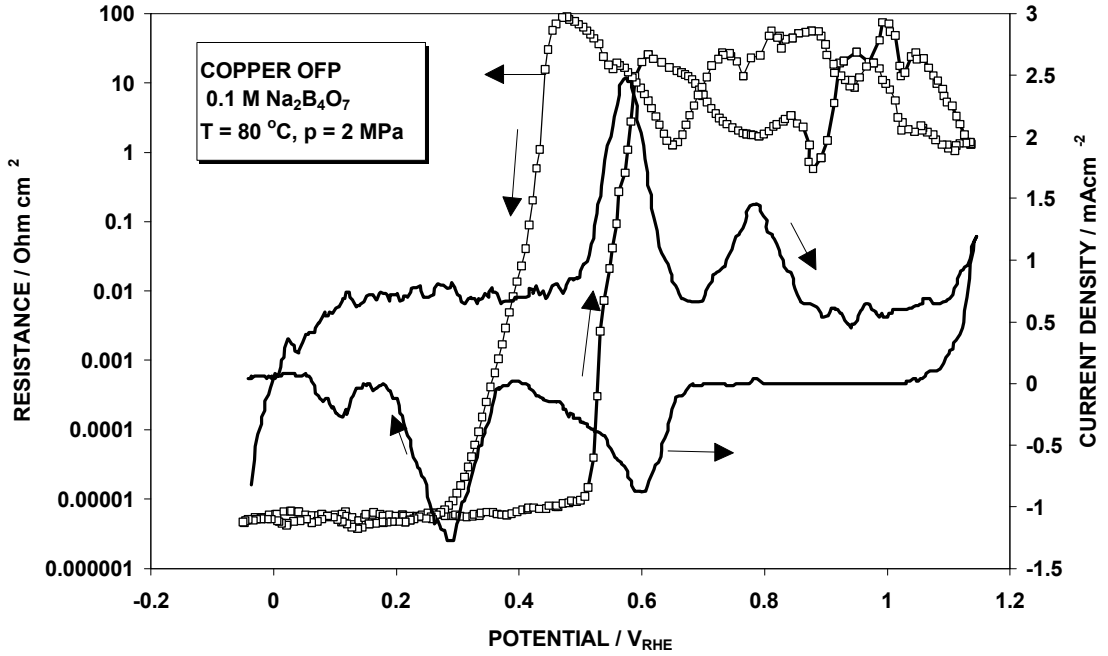

Figure 7. Contact electric resistance (symbols) and current density (line) of Cu OFP as a function of potential. Sweep rate 0.1 mV/s.

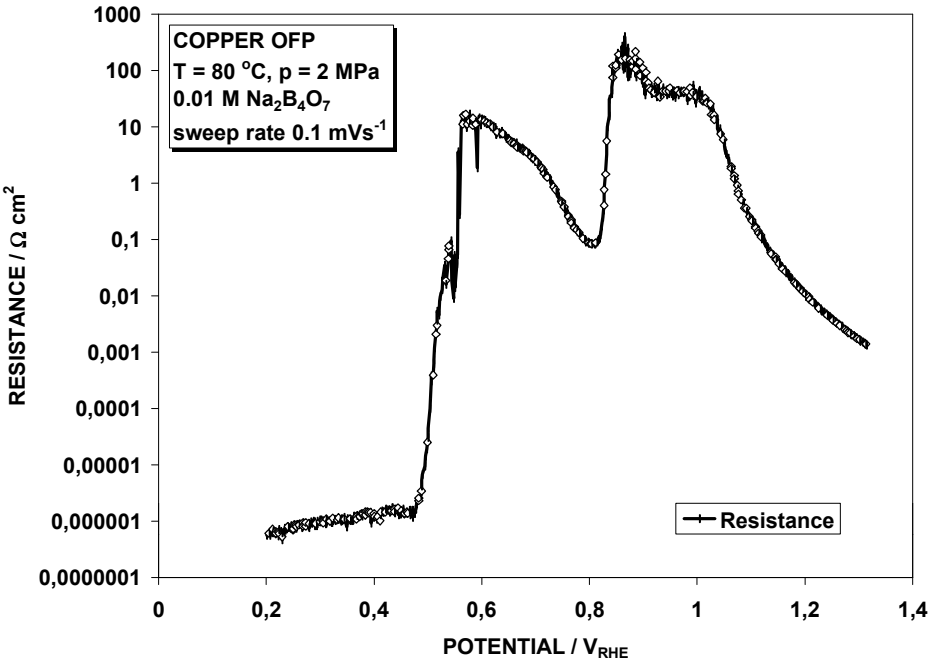

Figure 8. The film resistance as a function of potential in a 0.01 M tetraborate solution.

4.3.3 Impedance response of the films on copper

The semiconductor properties of the oxide films on copper were investigated by measuring the capacitance of the specimen during a negative going potential sweep. The result in the form of C^{-2} versus electrode potential -plots for oxide films formed at 0.6 V_{RHE} and at 1.3 V_{RHE} are shown in Fig. 9. The capacitance of the film formed at 1.3 V_{RHE} remained constant at potentials where divalent copper oxide (mostly CuO) is stable, i.e. $E > 0.75\ V_{RHE}$, indicating that the film shows no semiconductor behaviour. However, the capacitance of the film that was formed at 0.6 V_{RHE} (mostly monovalent copper oxide, Cu_2O) showed a decreasing capacitance (linearly increasing C^{-2} as a function of decreasing potential) in the potential range $0.55\ V_{RHE} < E < 0.75\ V_{RHE}$. This indicates that the film that is mostly Cu_2O shows p-type semiconductor properties.

To determine the semiconductor characteristics of the film formed in the monovalent copper oxide region, the space charge layer capacitance was extracted from the data of Fig. 9 assuming that the capacitance at 0.0 V_{RHE} is equal to the Helmholtz layer capacitance of the copper/electrolyte interface. Plot of the inverse space charge layer capacitance squared vs. potential, i.e. Mott-Schottky -plot is shown in Fig. 10. It is well approximated with a straight line according to the following relationship valid for p-type semiconductors

$$C_{sc}^{-2} = (2/e\varepsilon\varepsilon_o N_A)(E_{fb} - E + kT/e) \qquad (9)$$

and the corresponding potential axis intercept furnishes an estimate of the flatband potential of the film: $0.82 \pm 0.01\ V_{RHE}$. From the slope of this dependence, using a value of 12 for the dielectric constant of Cu_2O [56], a value of the acceptor density is calculated as $n = 7 \cdot 10^{20}\ cm^{-3}$. This value is typical for anodically formed semiconductor films [56].

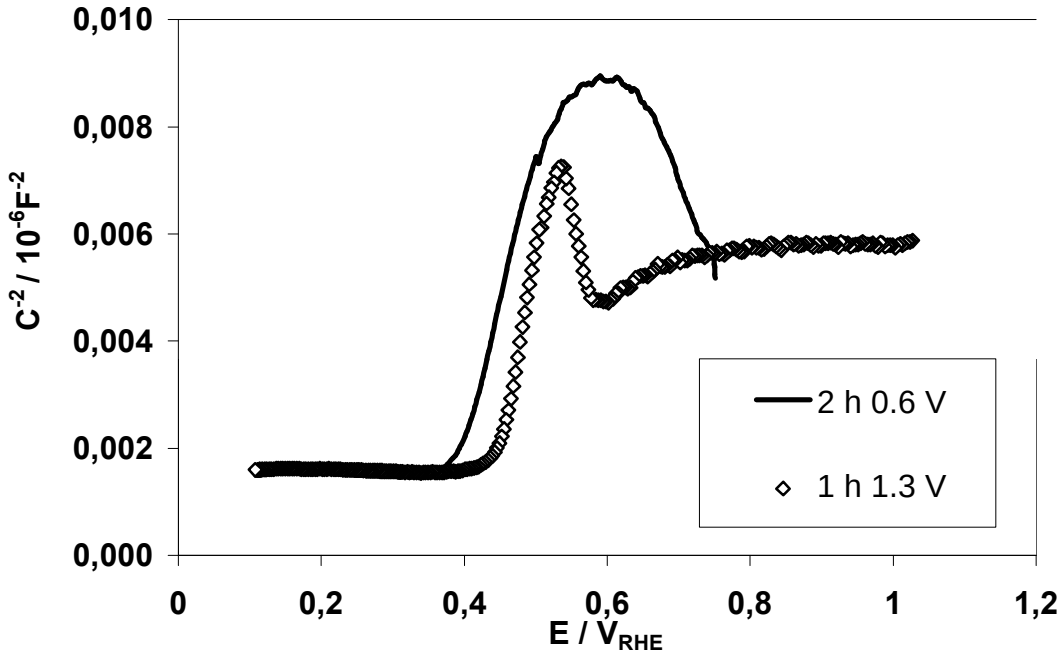

Figure 9. C^{-2} versus electrode potential for Cu OFP oxidised at 0.6 V_{RHE} and at 1.3 V_{RHE}.

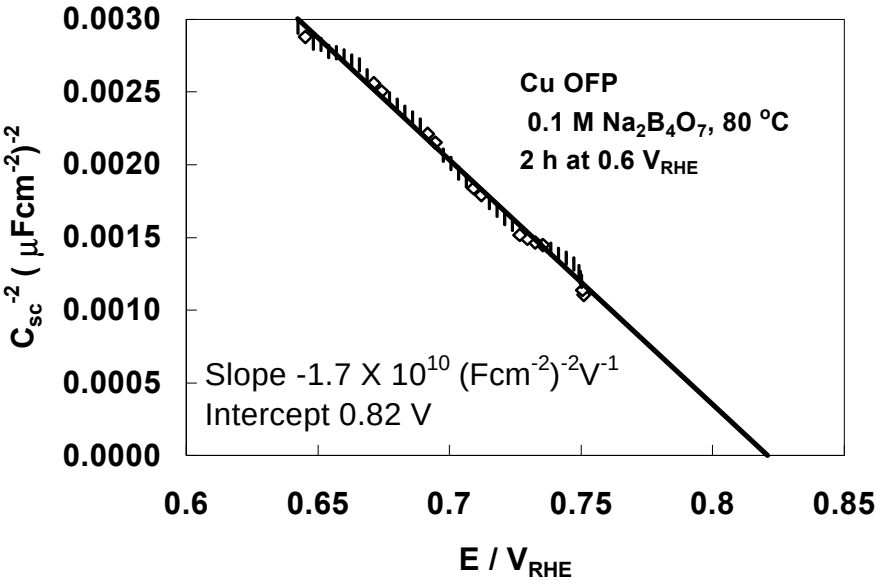

Figure 10. Mott-Schottky plot for a film grown at +0.60 V_{RHE} on Cu OFP in 0.1 M $Na_2B_4O_7$ at 80°C.

For a p-type semiconductor, the width of the space charge layer is a function of the acceptor density and the potential drop, i.e

$$W = (2\varepsilon\varepsilon_O/eN_A)^{0.5} (E_{fb} - E)^{0.5} \quad (10)$$

From this equation, the space charge layer thickness, i.e. the thickness of the semiconducting part of the surface film becomes $W = 8*10^{-10}$ m at E = 0.6 V_{RHE}. It is clear that the semiconducting part of the film is only a small fraction of the total film thickness shown in Fig. 6.

From general grounds, it is very likely that the corrosion rate of a metal covered with a surface film exhibiting semiconductor or insulator properties is limited by the transport of metal ions through it. Thus factors influencing the electrical and transport properties of the surface film most probably have a great impact on the corrosion rate. In order to investigate the role of different conditions for film formation on copper, impedance spectroscopic measurements in 0.1 M $Na_2B_4O_7$ were performed in two ways:

- Starting from a fresh, mechanically ground surface, reducing the airborne film at -0.2 V vs. RHE for 30 min and forming an anodic film by potentiostatic polarisation of the copper electrode at 0.6 or 0.75 V vs. RHE for 3...20 h. Measuring the impedance response during film formation.
- Simulation of a cyclic oxidising / reducing / oxidising condition by performing a series of cyclic potentiodynamic sweeps (potential range -0.2 / 1.2 / -0.2 V vs. RHE, sweep rate 0.1 and 1 mVs^{-1}), reducing the formed film at -0.2 V vs. RHE for 30 min and forming an anodic film by potentiostatic polarisation of the copper electrode at 0.6 or 0.75 V vs. RHE for 3..20 h. Measuring the impedance response during film formation.

Fig. 11 shows the electrochemical impedance spectra of Cu oxidised at 0.6 V and Fig. 12 the spectra of Cu oxidised at 0.75 V for 3…20 h following the first experimental procedure. The results point to two dominating processes in the stability region of monovalent copper. The process resulting in the time constant at higher frequencies could be related to the electronic properties of the semiconductor part of the film, while that at lower frequencies is a combination of a interfacial charge transfer and a transport process.

The spectra shown in Figs. 11 and 12 can be successfully described with the following equivalent circuit

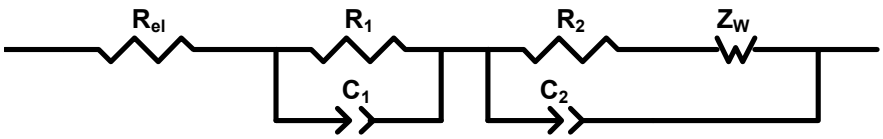

where R_{el} is the electrolyte resistance, R_1 and C_1 are the semiconductor layer resistance and capacitance, respectively, R_2 is the charge transfer resistance and C_2 the interfacial capacitance.

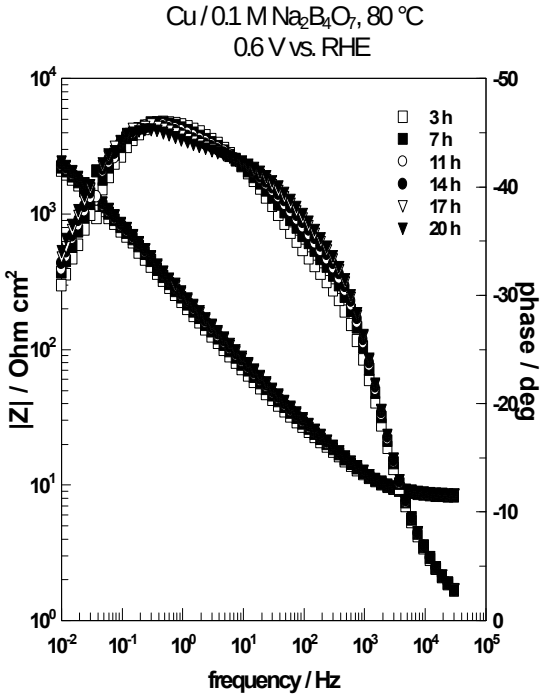

Figure 11. Impedance spectra for Cu OFP oxidised in 0.1 M $Na_2B_4O_7$ ($T = 80^oC$, $p = 2$ MPa) at $E = 0.6\ V_{RHE}$. Oxidation of fresh surface.

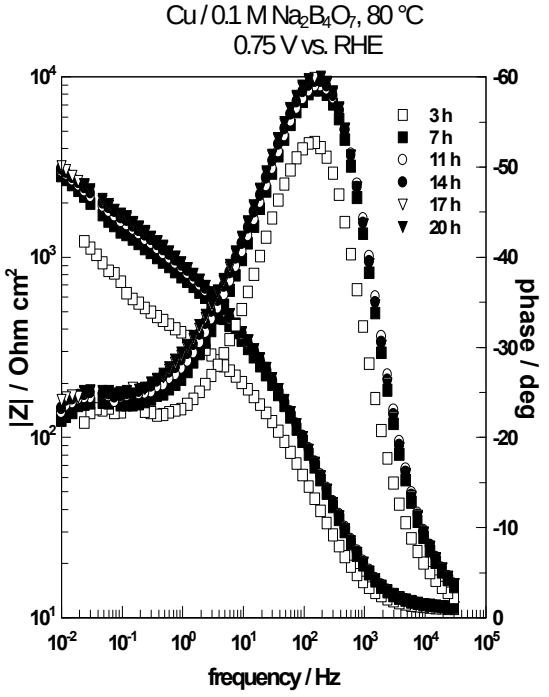

Figure 12. Impedance spectra for Cu OFP oxidised in 0.1 M $Na_2B_4O_7$ ($T = 80^oC$, $p = 2$ MPa) at $E = 0.75\ V_{RHE}$. Oxidation of fresh surface.

Here Z_w is a Warburg impedance described by the function

$$\mathbf{Z_W} = \mathbf{R_W} \tanh\ [(j\omega\tau_W)^{0.5}]\ /\ (j\omega\tau_W)^{0.5}$$

where $\mathbf{R_W}$ is the transport resistance and τ_W is the time constant of the transport process. As the transport process can be described by a finite-length Warburg impedance, it most probably occurs in the semiconductor part of the anodic film. The best-fit values of the parameters $\mathbf{R_W}$, τ_W, R_1,C_1,R_2 and C_2 are collected in Table IV for the two potentials at which the measurements were carried out.

Table IV. *Fitting parameters for Cu OFP oxidised in pure tetraborate solution for 3 20 hrs at +0.6 V_{RHE} (a) and +0.75 V_{RHE} (b).*

(a)
0.6 V RHE

Time / h	$R_1/\Omega cm^2$	$C_1/\mu Fcm^{-2}$	$R_2/\Omega cm^2$	$C_2/\mu Fcm^{-2}$	$R_W/\Omega cm^2$	τ_W /s
3	15	13.6	429	370	4900	72
7	12.2	15.0	1060	320	4850	156
11	19	12	1432	440	6400	200
14	10	14.5	1364	490	10400	400
17	13	14	1419	270	6700	400
20	12.2	13.7	1060	193	7500	400

(b)
0.75 V RHE

Time / h	$R_1/\Omega cm^2$	$C_1/\mu Fcm^{-2}$	$R_2/\Omega cm^2$	$C_2/\mu Fcm^{-2}$	$R_W/\Omega\ cm^2$	τ_W /s
3	93	19	234	39	2210	16.4
7	160	12	512	23	6540	64
11	150	11	450	21	9550	190
14	155	11.5	440	21	12250	400
17	150	12.8	490	19	13200	400
20	150	12.6	450	20	13220	400

The following conclusions can be made from the data in Table IV:

- The rate of the ionic transport process (inversely proportional to the transport resistance R_W) which is likely to be the limiting step in the corrosion reaction is practically the same for both potentials. The resistance R_W does not change very much with the time of oxidation at 0.6 V and increases up to 14 h of oxidation at 0.75 V.
- The time constant of the transport process τ_W increases up to 14 h of oxidation and preserves a constant value for longer times. As this time constant can be described with the equation $\tau_W = \delta^2 / D$, where δ is the thickness of the layer in which the transport occurs and D is the diffusion coefficient of the transported ionic species, this probably means that for oxidation times longer than 14 h the thickness of the barrier part of the anodic layer does not change any more.

- The rate of the interfacial charge transfer reaction (inversely proportional to R_2) is ca. two times higher at 0.75 V than at 0.6 V. This is in good correlation with the higher steady state current density measured at 0.75 V when compared to 0.6 V.
- The capacitance of the semiconductor layer C_1 is practically the same for both potentials whereas its resistance is much higher at 0.75 V than at 0.6 V. At present, no clear explanation of this observation can be given.

Figure 13 shows the electrochemical impedance spectra of Cu oxidised at 0.6 V and Fig. 14 that of Cu oxidised at 0.75 V for 3…20 h following the second experimental procedure. It turned out that these spectra although quantitatively different from those obtained using the first experimental procedure, contain the same number of time constants and can be described using the same equivalent circuit. This is a good indication that the experimental procedure does not change fundamentally the nature of the processes controlling the impedance response of the copper / anodic film / solution system.

The best-fit values of the parameters R_W, τ_w, R_1,C_1,R_2 and C_2 are collected in Table V for the two potentials at which the measurements were carried out.

The following conclusions can be made:

- The rate of the transport process is significantly greater for the film formed at 0.75 V when compared to that formed at 0.6 V. Furthermore, a significant increase of the transport resistance with the time of oxidation at 0.6 V is observed indicating the formation of a film which is the less defective, the longer the oxidation time. This result is in accordance with the fact that the time constant of the transport process is roughly 4 times smaller than in the case of films formed according to the first experimental procedure (cf. Tables IV and V). This indicates that probably the thickness of the barrier part of the layer is smaller in the case of the films formed according to the second experimental procedure. It is likely that less defective films will grow to a smaller thickness, because of the lower ionic defect transport rate.
- The charge transfer resistance R_2 is once again ca. 3 times smaller at 0.75 V indicating a faster rate of the charge transfer reaction at this potential.
- The capacitance of the semiconductor part of the layer C_1 for the films formed according to the second experimental procedure is significantly smaller at 0.6 V when compared to 0.75 V. This may mean that the semiconductor part of the film at 0.6 V is thicker or has a smaller dielectric constant. Another important feature is that the capacitance C_1 decreases with the time of oxidation at 0.6 V and stays roughly constant at 0.75 V. The values of this capacitance at 0.75 V are close to a typical value for the Helmholtz layer capacitance, i.e. the thickness of the semiconducting part of the layer is less than a monolayer. This fact is in correlation to the result that the resistance of the semiconducting part of the layer R_1 is significantly smaller for films formed at 0.75 V than at 0.6 V and decreases with the oxidation time.

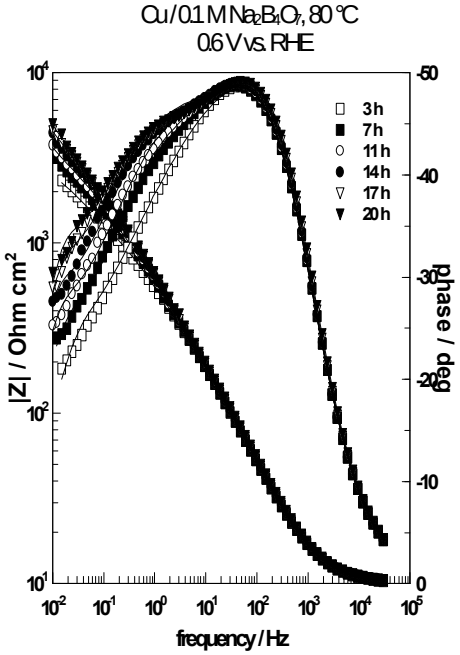

Figure 13. Impedance spectra for Cu OFP oxidised in 0.1 M $Na_2B_4O_7$ ($T = 80^oC$, $p = 2$ MPa) at $E = 0.6\ V_{RHE}$. Oxidation of surface after cyclic sweeps.

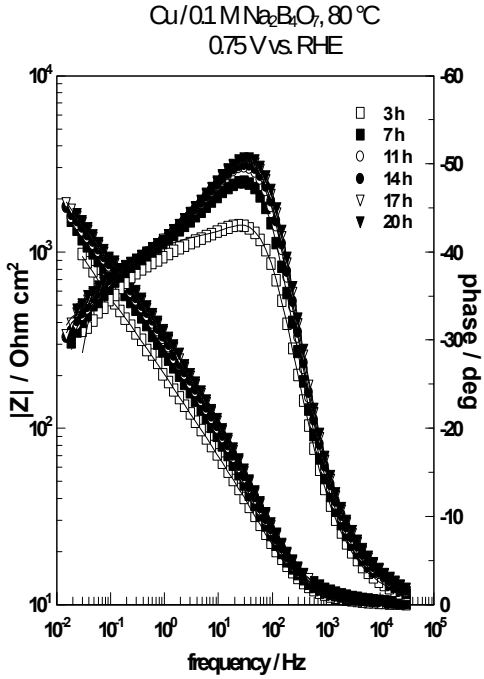

Figure 14. Impedance spectra for Cu OFP oxidised in 0.1 M $Na_2B_4O_7$ ($T = 80^oC$, $p = 2$ MPa) at $E = 0.75\ V_{RHE}$. Oxidation of surface after cyclic sweeps.

Table IV. *Fitting parameters for Cu OFP oxidised after cyclic sweeps in pure tetraborate solution for 3 20 hrs at +0.6 V_{RHE} (a) and +0.75 V_{RHE} (b).*

(a)

0.6 V RHE

Time / h	$R_1/\Omega cm^2$	$C_1/\mu Fcm^{-2}$	$R_2/\Omega cm^2$	$C_2/\mu Fcm^{-2}$	$R_W/\Omega\ cm^2$	τ_W /s
3	110	12.4	433	52	5300	55.7
7	128	6.15	577	76	7800	81.1
11	115	7.12	754	43	9300	93.8
14	101.5	10.6	1214	15	10120	84.1
17	132	5.36	700	80	13700	100
20	118	5.28	623	67	14020	77.5

(b)
0.75 V RHE

Time / h	$R_1/\Omega cm^2$	$C_1/\mu Fcm^{-2}$	$R_2/\Omega cm^2$	$C_2/\mu Fcm^{-2}$	$R_W/\Omega\ cm^2$	τ_W /s
3	38	76.7	112.5	80	2200	18.8
7	39.5	103	206	310	3560	36.5
11	36	58	360	165	6656	100
14	16.5	68	260	190	5260	71.2
17	14	58	227	190	5920	79
20	15	56	330	120	7800	143

The results shown above give rise to a physical model for the structure of the surface film forming on copper at potentials where monovalent copper is stable. The film thickness calculated from the reduction charge was of the order of 10^{-6} m. However, the capacitance values measured indicate that the semiconducting layer of the film has a thickness of the order of 10^{-9} m. The model shown in Fig. 15 describes the film as consisting of a thin semiconducting layer at the film/electrolyte -interface and a thick inner layer. The location of the thin semiconducting layer is suggested to be at the film/electrolyte -interface, although it is realised that the location is influenced by the ratio of the rate of the formation of cation vacancies at the film/electrolyte -interface and the rate of formation of oxygen vacancies at the metal/film -interface.

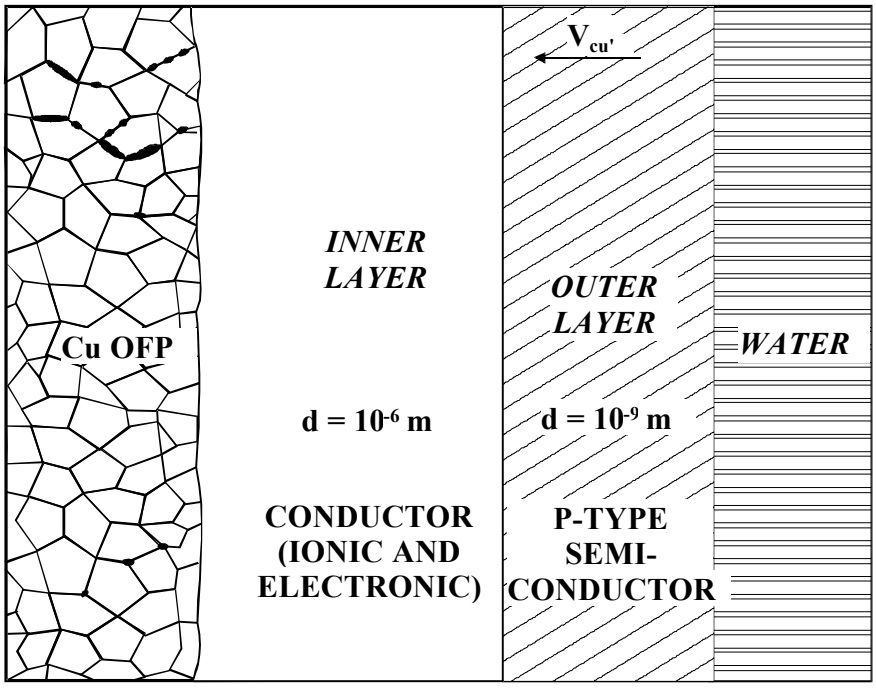

Figure 15. A physical model of the structure of surface films forming on copper in 0.1 M $Na_2B_4O_7$ at 80 °C and in the potential range where monovalent copper is stable.

4.4 Conclusions

The surface film forming on Cu OFP in 0.1 M $Na_2B_4O_7$ at T = 80 °C in the stability region of monovalent copper oxide can be described to consist of a bulk film and a thin outer layer. The bulk film has a thickness of about 10^{-6} m and it is a good electronic and ionic conductor. The thin outer layer at the film/electrolyte interface has a thickness of about 10^{-9} m, and shows p-type semiconductor properties. In the stability range of divalent copper the bulk film has the same thickness and is also a good electronic and ionic conductor. The thin outer layer does not show semiconductor properties. The rate of oxidation of copper, i.e. the corrosion rate of copper is controlled by the transport of cation vacancies in the thin outer layer both in the stability region of monovalent and divalent copper.

5 SUMMARY OF RESULTS IN BORAX SOLUTION WITH CHLORIDES

5.1 INTRODUCTION

In borax solution containing chloride ions CuCl is supposed to precipitate on the Cu_2O layer. At higher potentials the structure of the surface film on copper has been suggested to be best represented by a hydrous inner Cu_2O layer non-homogeneously covered by $Cu(OH)_2$ and CuCl precipitates [49].

n-type semiconductive characteristics have been observed when copper was immersed in 0.1 M NaCl solution, which was probably due to the formation of a CuCl layer on top of the Cu_2O film [60]. A similar structure has been suggested in the presence of chlorides in weakly acidic [61] and alkaline [62] solutions. Cu_2O can be formed on copper in the presence of chlorides at any pH [62]. Modestov et al. [62] suggest that CuCl also affects the semiconductive properties of Cu_2O by doping it with Cl^- ions.

5.2 Experimental

The effect of chlorides on surface films and electrochemical behaviour of copper was studied in 0.01 M and 0.1 M $Na_2B_4O_7$ electrolyte. Chloride additions were made in the form of NaCl. In other respects the experimental conditions were similar to those described earlier for tests conducted in 0.1 M $Na_2B_4O_7$ electrolyte, see section 4.2.

5.3. Results and discussion

5.3.1. Resistance-potential curves

The film resistance together with the polarisation current of the CER tips measured at 80°C in 0.01 M tetraborate + 0.03 M NaCl solutions is shown in Fig 16. Measurements in 0.1 M tetraborate solution were unsuccessful because of what was interpreted as formation of slime-like electrically conducting substance between the closely separated CER tips.

In 0.01 M tetraborate solution containing chlorides, a dramatic decrease in resistance was observed when the potential reached the value of approximately +0.8 V_{RHE} during the sweep in the positive direction as shown in Fig. 16. A strong increase in the anodic current was observed at about the same potential. No significant increase of resistance was observed at higher potentials. At lower potentials in the stability region of monovalent copper the resistance was higher by roughly one decade than in the same solution without chlorides, see Fig. 8. These results indicate that chloride ions have a detrimental influence on the film on copper in the stability region of Cu(II), while they exert only a minor influence on a film formed in the stability region of monovalent copper, Cu(I).

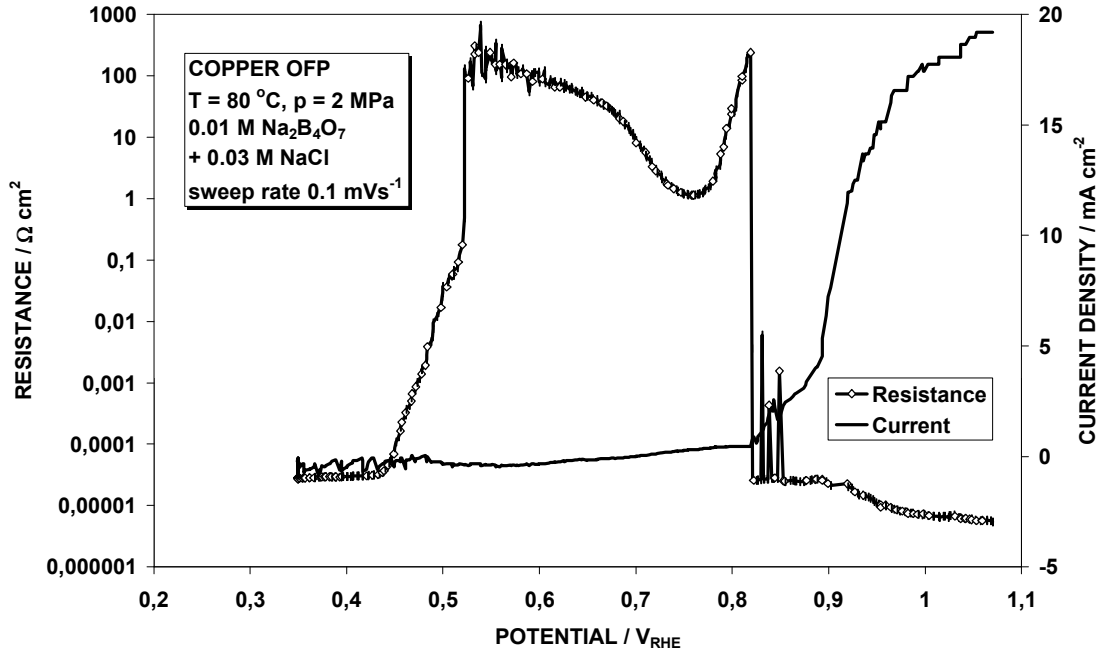

Figure 16. The film resistance and the current density of the CER specimens measured as a function of potential in a solution containing 0.01 M tetraborate + 0.03 M NaCl.

5.3.2 Addition of chlorides on steady state films formed in chloride-free solutions

The effect of chloride ions on the stability of steady state surface films grown both in the stability region of monovalent (at +0.60 V_{RHE}) and in the stability region of divalent copper (at +1.00 V_{RHE}) in chloride free 0.01 M tetraborate solution was studied at 80°C.

An addition of 0.03 M and a subsequent addition of 0.07 M chlorides in electrolyte did not affect the film resistance (ca. 200 Ωcm^2) of a film grown for 17 hours in the stability region of monovalent copper (mainly Cu_2O) in 0.01 M $Na_2B_4O_7$ at +0.60 V_{RHE}. A different behaviour was observed for films grown in the stability region of divalent copper (Fig. 17). The resistance of a film grown on Cu OFP for 18 hours at +1.00 V_{RHE} in 0.01 M $Na_2B_4O_7$ was approximately 2 Ωcm^2 before the NaCl injection of 0.03 M as shown in Fig. 17. The chloride injection increased the polarisation current of the CER specimens significantly, but no changes in the film resistance were observed during the first hours since the start of the injection. However, after an exposure of approximately five hours to the chlorides, the film converted first to an insulator for less than a one minute, which was followed by an abrupt film resistance decrease of eight orders of magnitude. Simultaneously the polarisation current increased again.

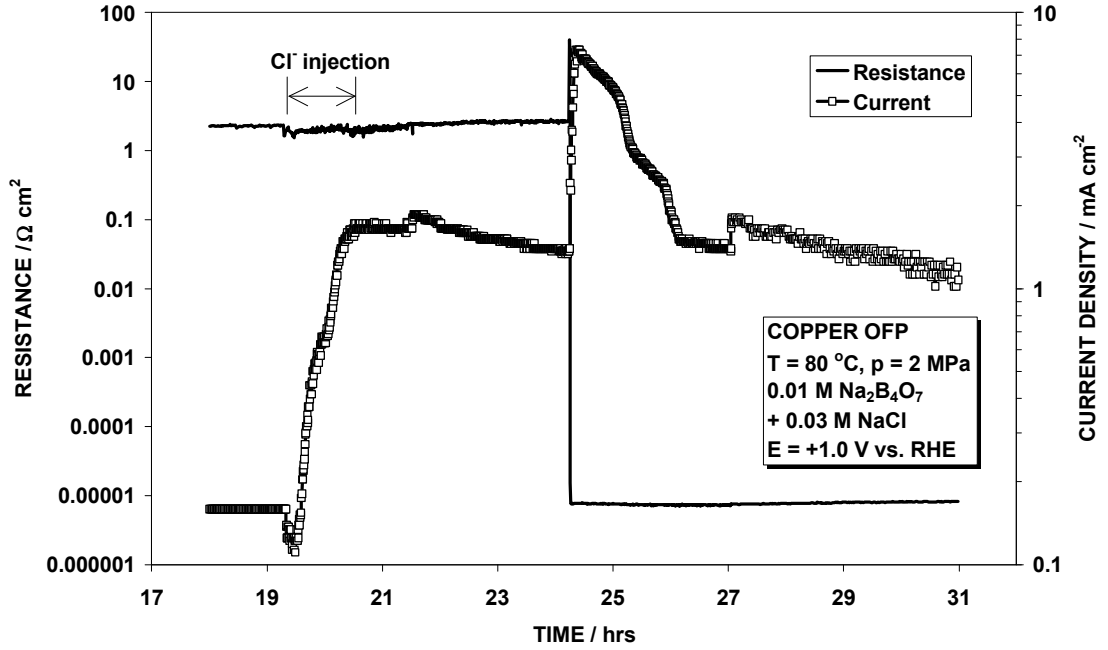

Figure 17. The effect of NaCl injection on the resistance and on the current density of the CER specimens for a film grown for 18 hours on Cu OFP in the stability region of divalent copper (at +1.0 V_{RHE}) in 0.01 M tetraborate solution. The total NaCl concentration was 0.03 M, and it was injected during the time period from 1 hour to 2 hours.

These results indicate that also in the case of steady state films chloride ions greatly influence the stability and the properties of the anodic film formed in the stability region of divalent copper.

5.3.3. Impedance response of the films on copper

Figure 18 shows the electrochemical impedance spectra of Cu OFP after 2 h oxidation in the potential region where divalent copper oxide is stable (1.0 V_{RHE}) and in the potential region where monovalent copper oxide is stable (0.6 V_{RHE}), both measured in 0.1 M $Na_2B_4O_7$ + 0.03 M NaCl.

The spectrum measured at +0.6 V_{RHE} is to a certain extent similar to that measured in pure borax without the presence of chlorides, see Fig. 11, although the impedance is clearly smaller and the transport process is not detected. The spectrum measured at +1.0 V_{RHE} shows one time constant at high frequencies probably related to the electronic conduction process and an additional time constant at low frequencies which probably describes the mass transfer through a porous layer. Moreover, the magnitude of the impedance at $f \rightarrow 0$ at +1.0 V_{RHE} was found to be ca. 1.5 decades lower in the solution containing Cl^- ions than in the pure tetraborate solution, once again in agreement with the CER results. This is probably due to the enhanced rate of the charge transfer reaction of copper oxidation by some chloride-assisted localised corrosion mechanism.

More information on the electronic properties of the surface films was gained by registering the capacitance of the Cu electrode during negative potential sweeps after 2 h

of oxidation in the potential regions of the stability of monovalent (0.6 V_{RHE}) and divalent (1.0 V_{RHE}) copper oxides in the 0.1 M $Na_2B_4O_7$ + 0.03 M NaCl solution. Such sweeps are shown in Mott-Schottky coordinates in Figure 19 (a). Similar data is presented for the 0.1 M $Na_2B_4O_7$ solution without the presence of chlorides in Fig. 9. It can be concluded that the anodic film formed in the stability region of monovalent copper (0.6 V_{RHE}) exhibits p-type semiconductor properties both in the Cl^- free and Cl^- containing solution as the inverse capacitance squared increases with the potential decreasing from 0.7 to 0.5 V_{RHE}. The subsequent decrease of this parameter is related to the reduction of the Cu(I) in the film to metallic copper. The film grown in the stability region of divalent copper (1.0 V_{RHE}) has no clear semiconductor properties since the square of the inverse capacitance stays rather constant in the range 0.7 to 1.0 V_{RHE} both in the Cl^- free and Cl^- containing solutions.

To determine the semiconductor characteristics of the film formed in the monovalent copper oxide region, the space charge layer capacitance was extracted from the data of Fig. 19 (a) assuming that the capacitance at 0.0 V_{RHE} is equal to the Helmholtz layer capacitance of the copper/electrolyte interface. Plots of the inverse space charge capacitance squared vs. potential were well approximated with straight lines according to the equation (9) presented above, as shown in Fig. 19 (b).

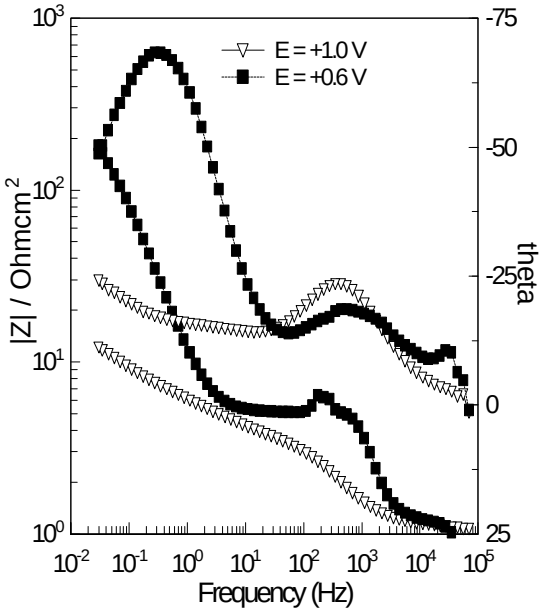

Figure 18. Impedance spectra of Cu OFP after 2 h oxidation in the potential region where divalent copper oxide is stable (1.0 V_{RHE}) and in the potential region where monovalent copper oxide is stable (0.6 V_{RHE}), 0.1 M $Na_2B_4O_7$ + 0.03 M NaCl.

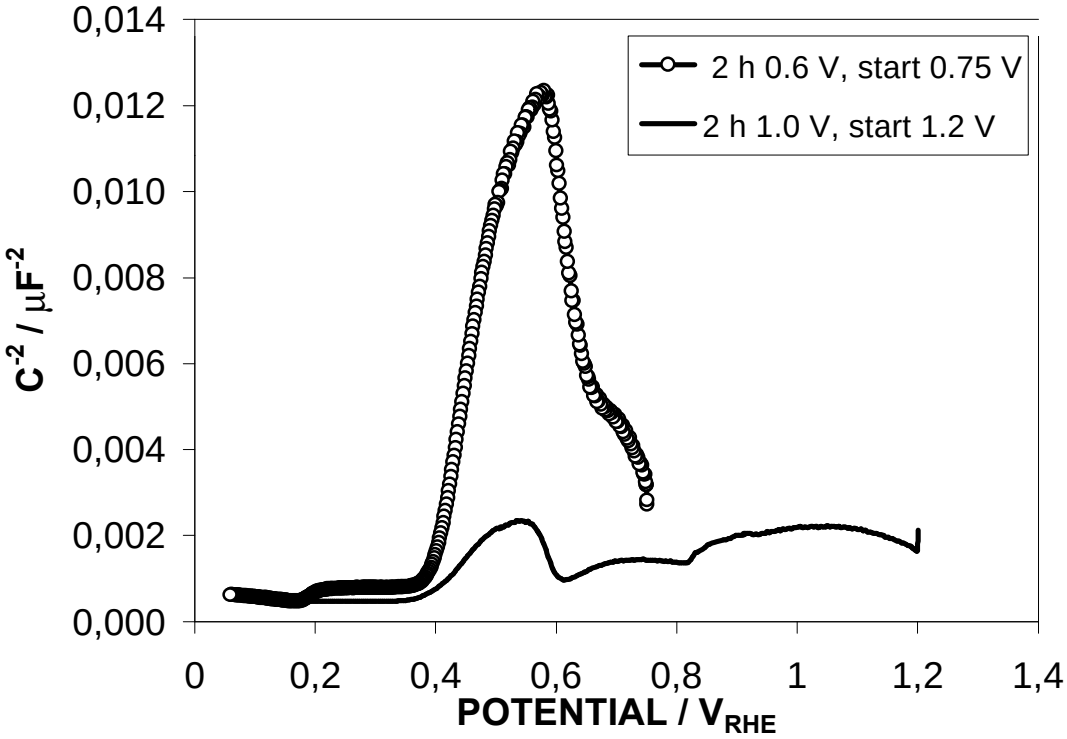

(a)

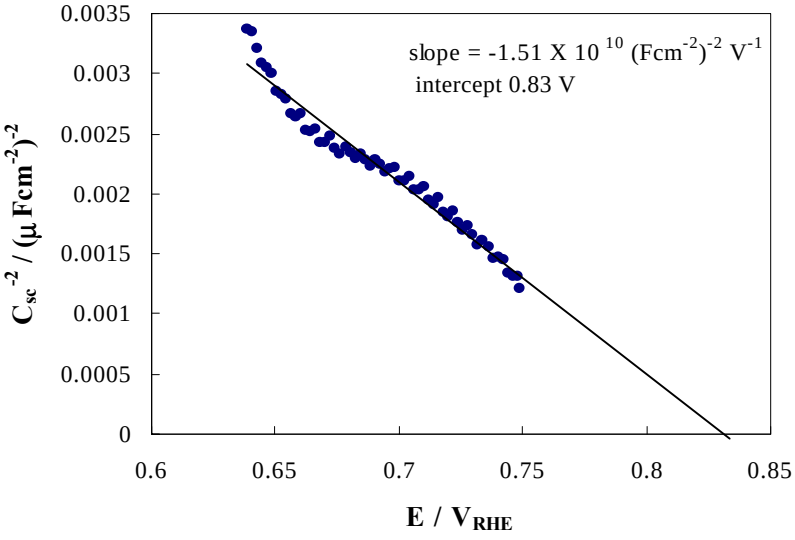

(b)

Figure 19. Inverse of capacitance squared, C^{-2} versus electrode potential for (a) monovalent and divalent oxides grown on Cu OFP in 0.1 M $Na_2B_4O_7$ + 0.03 M NaCl at 80°C and (b) the space charge layer (Mott-Schottky plot) of a film grown at +0.60 V_{RHE}.

The corresponding intercept with the potential axis furnishes an estimate of the flatband potential of the film at 0.82 ± 0.01 V_{RHE} (Fig. 19b),. From the slope of this dependence, using a value of 12 for the dielectric constant of Cu_2O [56] the value of the acceptor density becomes $N_A = 8 \cdot 10^{20}$ cm^{-3} for the 0.1 M $Na_2B_4O_7$ + 0.03 M NaCl solution. This

value is slightly higher than the one estimated for the Cl^- free $Na_2B_4O_7$ solution earlier ($7 \cdot 10^{20}$ cm^{-3}). This may indicate that the film formed at +0.6 V_{RHE} in the solution containing chloride ions is slightly more defective than that formed without the presence of chlorides.

5.4. Conclusions

In the potential region of divalent copper, surface films formed in $Na_2B_4O_7$ solutions containing chloride ions were found to be prone to break down. The breakdown of the films was observed during potentiodynamic scans in the presence of chloride ions, as the film resistance abruptly decreased by several orders of magnitude at E > 0.7 V_{RHE}. Also, steady state films formed in chloride free $Na_2B_4O_7$ solution in the stability region of divalent copper broke down, when chloride ions were added afterwards to the solution. Impedance of the films formed in the presence of chlorides at +1.0 V_{RHE} was found to be more than a decade smaller than that of the films formed at +0.6 V_{RHE}. This indicates a markedly higher corrosion rate at the higher potential +1.0 V_{RHE}.

6. RESULTS IN BORAX SOLUTION WITH 10 PPM H_2S

6.1 Experimental

Tests were performed in an autoclave in 0.1 M 0.1 M $Na_2B_4O_7$ + 10 ppm hydrogen sulphide (H_2S) solution at 80°C temperature. Hydrogen sulphide was added by bubbling continuously through the solution a gas mixture of Ar + 3% H_2 + 350 ppm H_2S (supplied by AGA Ltd) at a pressure of 2 MPa. This gas mixture was calculated to give an equilibrium concentration of 10 ppm of dissolved H_2S in the water. All the tests were performed in a static nickel cladded autoclave. In other respects the experimental conditions were similar to those described earlier for tests conducted in 0.1 M $Na_2B_4O_7$ electrolyte, see section 4.2.

6.2 Results and discussion

6.2.1 Voltammetric measurements

The cyclic voltammogram in Fig. 20 shows the same features as the one measured in borax solution without H_2S. The peaks A_I and A_{II} are connected with the formation of monovalent and divalent copper, respectively. The peak A_{III} with its cathodic counterpart C_{III}, not seen in the solution without H_2S (Fig. 5) are suggested to be related to the formation and reduction of a higher valent copper species or e.g. peroxide incorporated in the Cu(II) matrix. During the positive going sweep with the scale used no clear peaks can be discerned in the potential

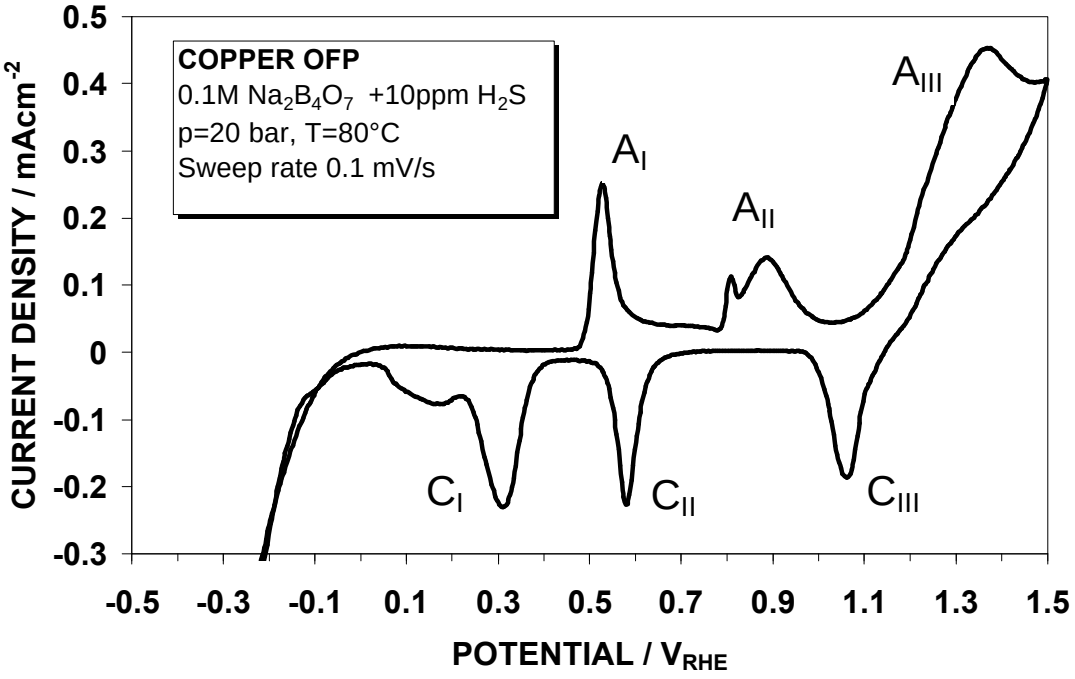

Figure 20. A cyclic voltammogram measured using a sweep rate of 0.1 mV/s.

range where copper sulphides are expected to form. However, using a finer scale, Fig. 21, reveals a very small peak located at about +0.1 V_{RHE}. This peak may be an indication of adsorption of a small amount of sulphide. The current density in the stability area of monovalent copper oxide does not increase as the potential is increased, which indicates that the rate limiting step of the oxidation reaction is not a charge transfer step. The same conclusion was made based on the voltammograms measured in borax solution without H_2S (see chapter 4.3.1). Increasing the sweep rate with a factor of 10 resulted in an increase in the current density, Fig. 22. However, the main features in the voltammogram remained relatively unchanged. The small anodic peak possibly related to sulphide adsorption on copper could be detected also with this sweep rate, Fig. 23. The peak potential was shifted towards higher potentials by about 0.05 V because of the higher sweep rate.

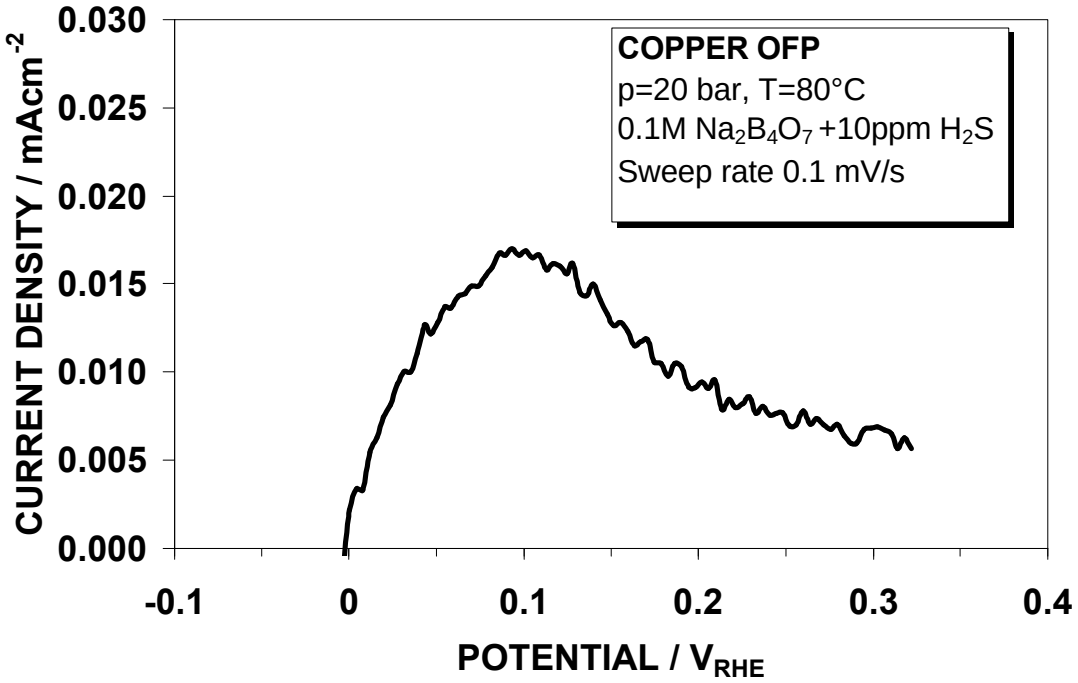

Figure 21. Fine scale detail of the cyclic voltammogram with sweep rate 0.1 mV/s.

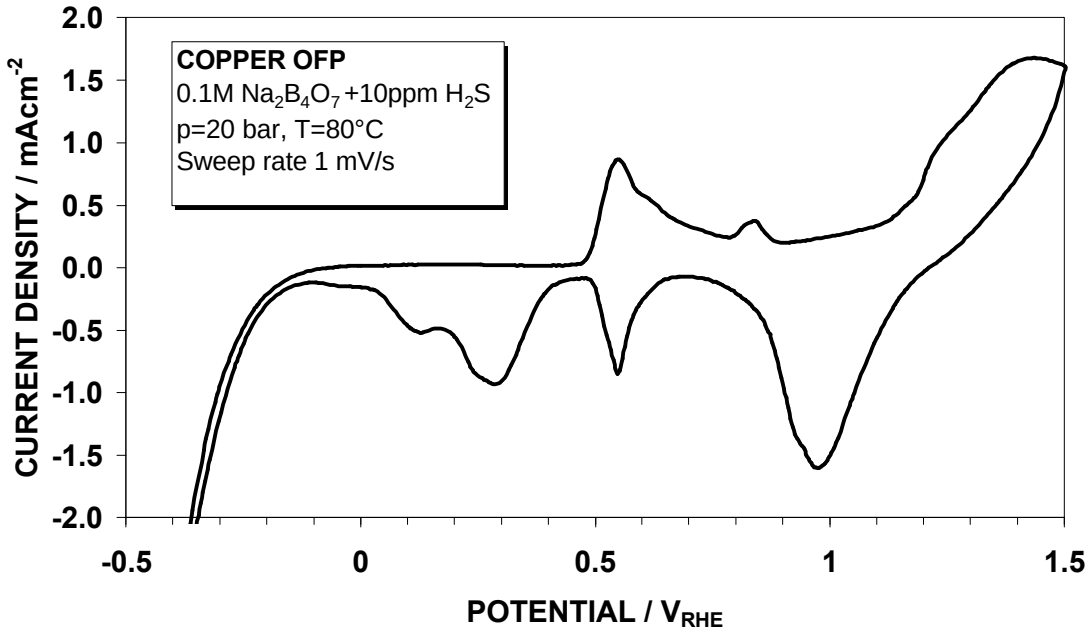

Figure 22. A cyclic voltammogram measured using a sweep rate of 1 mV/s.

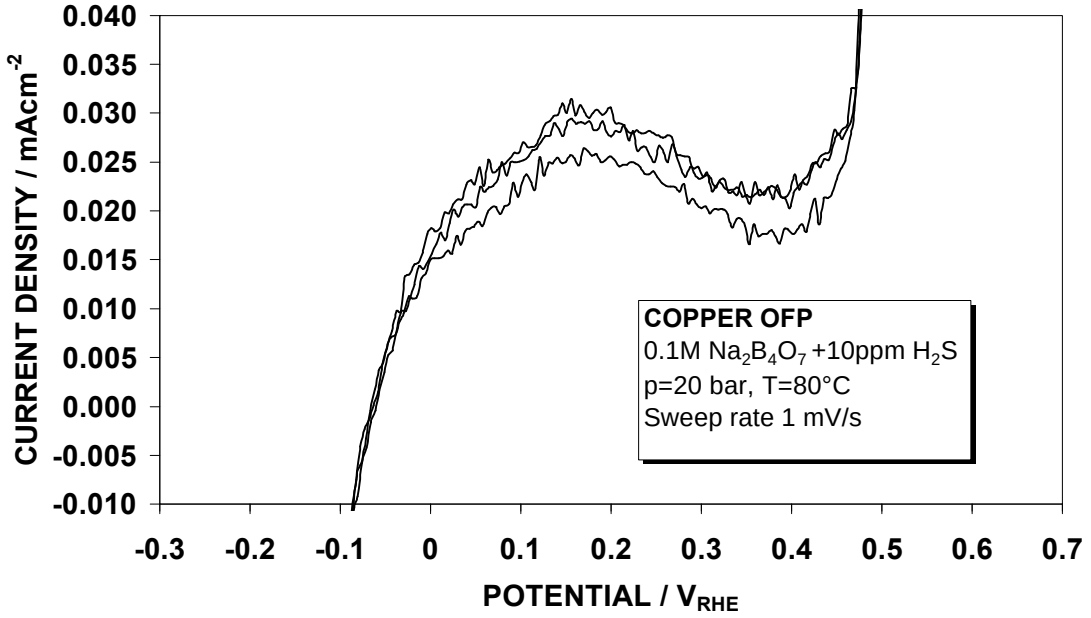

Figure 23. Three successive cyclic polarisation experiments showing a small anodic peak between 0 and +0.4 V.

The surface film thickness was calculated based on the charge consumed in reduction during a negative going sweep in the same way as for films grown in pure borax solution (chapter 4.3.1). An example of the reduction current densities as a function of potential is shown in Fig. 24. The average thickness is roughly a decade higher than that found for

films grown in solution without H_2S, see Fig. 6. This indicates that 10 ppm H_2S in solution increases markedly the growth rate of surface films on copper.

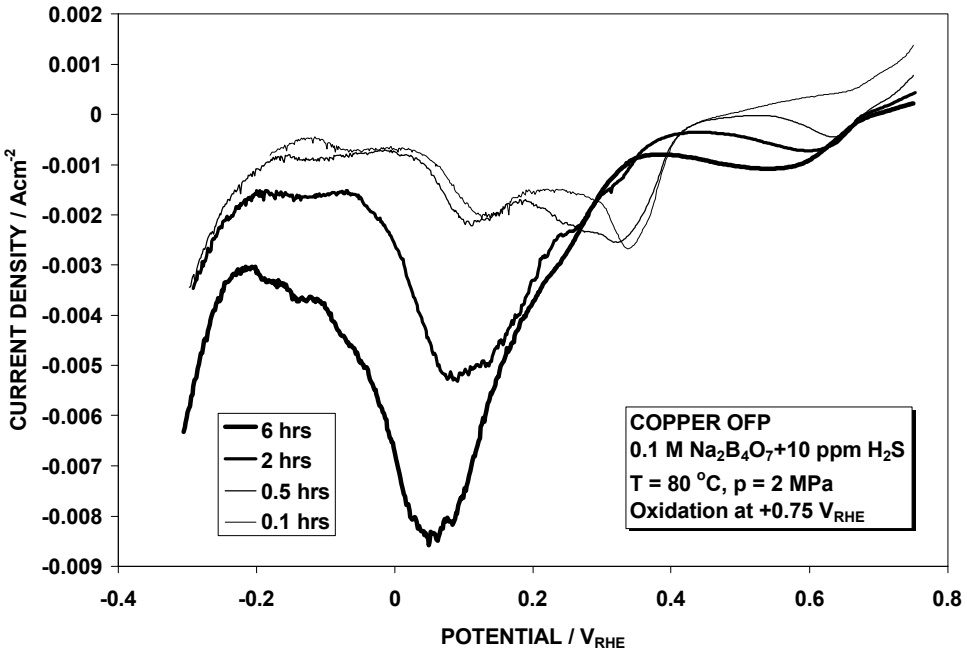

Figure 24. Current density as a function of potential during a negative going sweep after oxidation treatment at +0.75 V for different times. Sweep rate 0.1 mV/s.

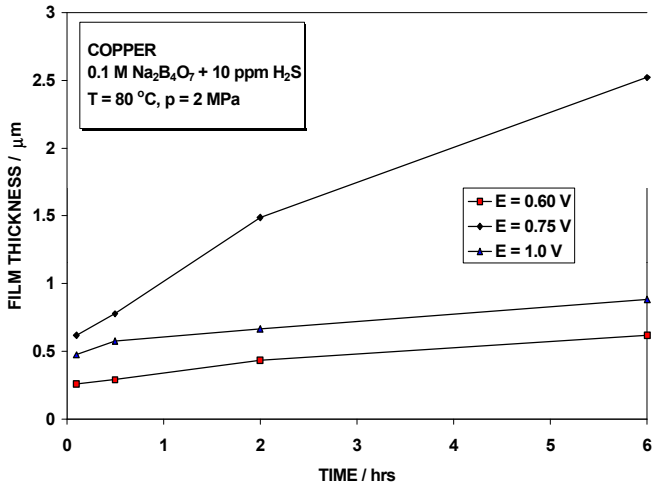

Figure 25. Surface film thickness as a function of oxidation time for Cu OFP in 0.1 M $Na_2B_4O_7$ and in 0.1 M $Na_2B_4O_7$ + 10 ppm H_2S.

6.2.2 Resistance - potential curves

The film resistance together with the polarisation current of the CER tips measured during a cyclic potential sweep from 0 V to +1.3 V and backwards is shown in Fig. 26. The observed behaviour of both resistance and current density resemble very closely that of Cu OFP in pure borax solution without the presence of sulphide (see chapter 4.3.2).

In the potential range where one may expect the formation of Cu_2S and CuS, i.e. -0.2 to +0.3 V_{RHE}, at the resolution level used (> 10^{-6} Ωcm^2) no peaks were detected in the resistance. In a separate experiment using an experimental arrangement allowing for higher resolution limit (>10^{-8} Ωcm^2) a small increase in resistance was detected starting from about -0.3 V, see Fig. 27. The resistance showed a small maximum at -0.05 V and a steadily increasing resistance from +0.1 V to +0.47 V at which potential oxide formation starts.

6.2.3 Resistance - time and potential - time curves

The surface film stability was further studied by monitoring the resistance and open circuit potential of a previously formed film. In the first experiment a specimen was oxidised in air for a day and then exposed to the environment in an autoclave while monitoring the open circuit potential. During the 14 day exposure the open circuit potential decreased from the starting value of 0.67 V to 0.63 V, indicating that an air formed oxide film is quite stable despite the rather high reducing power of the environment.

The evolution of potential and resistance in an experiment in which the film was formed and let reduce in an aqueous environment are shown in Fig. 28. The specimen was first polarised at 0 V in order to clean the surface, then polarised at +1.3 V to grow a surface film which was then let reduce under open circuit conditions. The resistance of the surface film at the end of the potentiostatic oxidation at +1.3 V was about $3*10^{-2}$ Ωcm^2 which is clearly lower than that shown in Fig. 26 for a film formed during a potential sweep in the corresponding potential range. This may indicate that the film formed at a constant potential (as shown in Fig. 28) is more defective than one forming in a slow potential sweep.

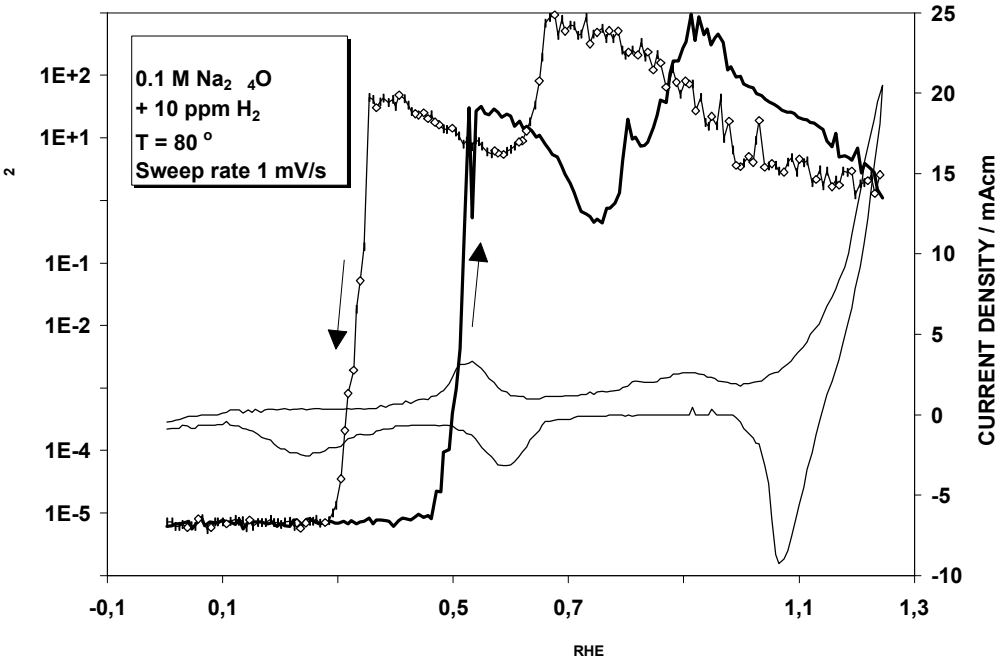

Figure 26. Resistance (positive going (thick black line) and negative going (symbols) sweeps) and current density (thin line) as a function of potential (sweep rate 1 mV/s).

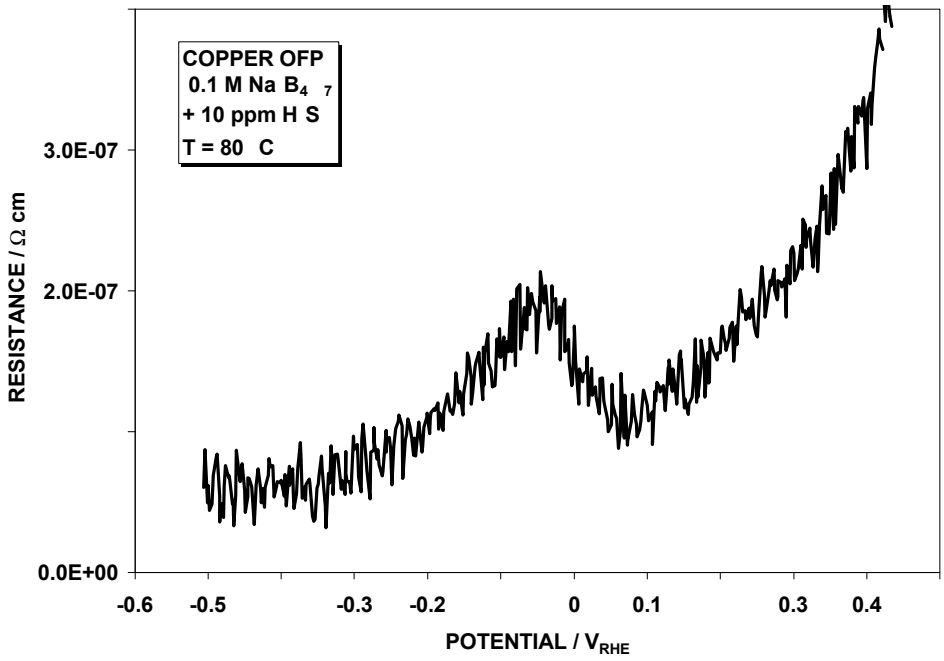

Figure 27. High resolution limit (>10^{-8} Wcm^2) measurement of the resistance at potentials where copper sulphide formation is expected to occur.

Three plateaus can be discerned in the open circuit potential vs. time curve, the first one at about +1.1 V, the second one at about +0.6 V and the third one at about +0.35 V. Such plateaus are thought to indicate the reduction of certain products with a certain

stoichiometry in the film, which need to be reduced before the potential may continue to decrease. The first plateau may be attributed to the reduction of high-valent copper or to that of peroxide incorporated in the film. During this reduction at about +1.1 V the resistance stays rather low, but during the decrease of the potential to the second plateau the value of the resistance increases. The second plateau is associated with the reduction of Cu(II) to Cu(I). When the potential decreases to the third plateau, which can be attributed to the reduction of Cu(I) to metallic Cu, the value of the resistance increases again. Finally, the resistance drops to values corresponding to a metallic surface.

This behaviour indicates that the resistance of the film is low when copper with two different oxidation states is present in the film in a significant amount. When mainly one oxidation state is present, the resistance exhibits high values. This can be explained in terms of conduction via a mechanism called polaron hopping. In polaron hopping an electron (or electron hole) jumps from one cation to another one, thus causing a change of oxidation state of both the cations. When considered in this way, a necessary condition for polaron hopping to occur is that there are (at least) two types of cations with different valence states present in the film. Thus high resistances can be expected when one oxidation state prevails, while lower resistances can be expected when two oxidation states are present.

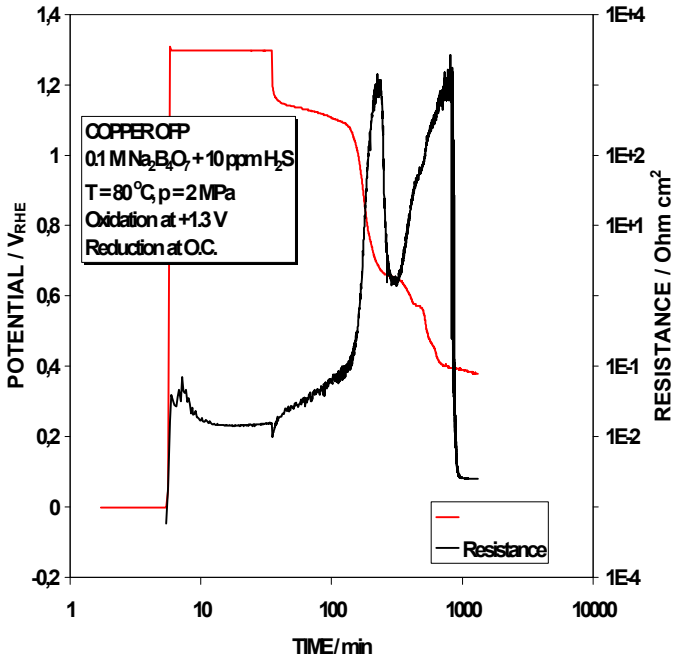

Figure 28. Resistance and potential as a function of time during three successive stages; reduction at 0 V, oxidation at +1.3 V and following reduction at open circuit.

In Fig. 29 the resistance is shown as a function of the open circuit potential from the same experiment as shown in Fig. 28. Comparing with the potentiodynamic reduction result shown in Fig. 26 (negative going sweep) the reduction process at open circuit conditions proceeds in a rather similar manner, indicating that the sweep rate used in the

potentiodynamic tests (1 mV/s) results in an almost steady state measurement. It is noteworthy that in the reduction process performed at open circuit conditions the final resistance level stayed at a level higher than 10^{-3} Ωcm^2, indicating that the surface did not reach the resistance level of an electrochemically cleaned surface (10^{-5} Ωcm^2).

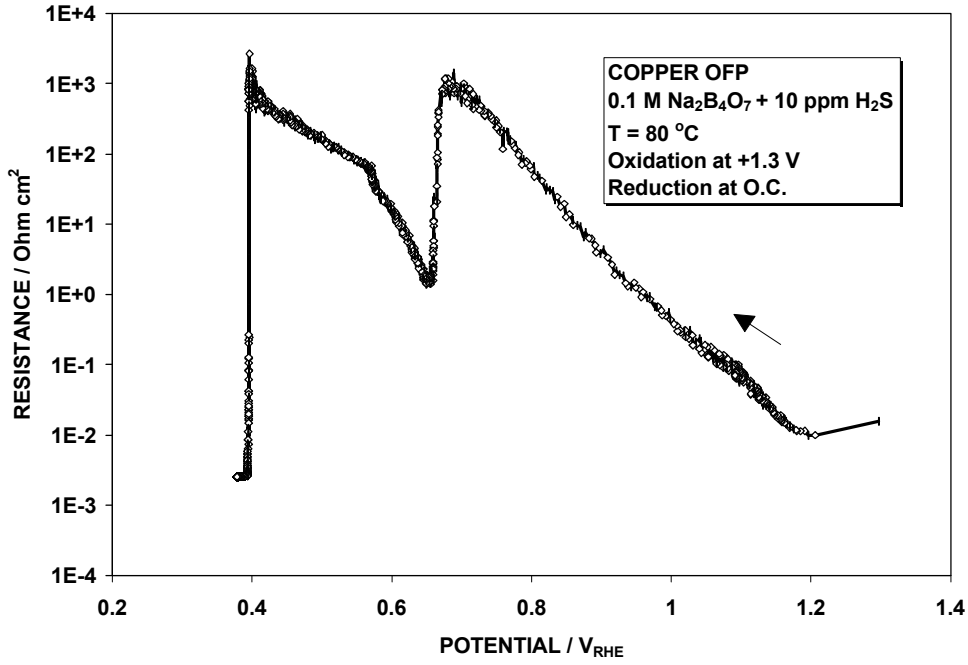

Potential dependence of resistance during reduction at open circuit after oxidation at +1.3 V.

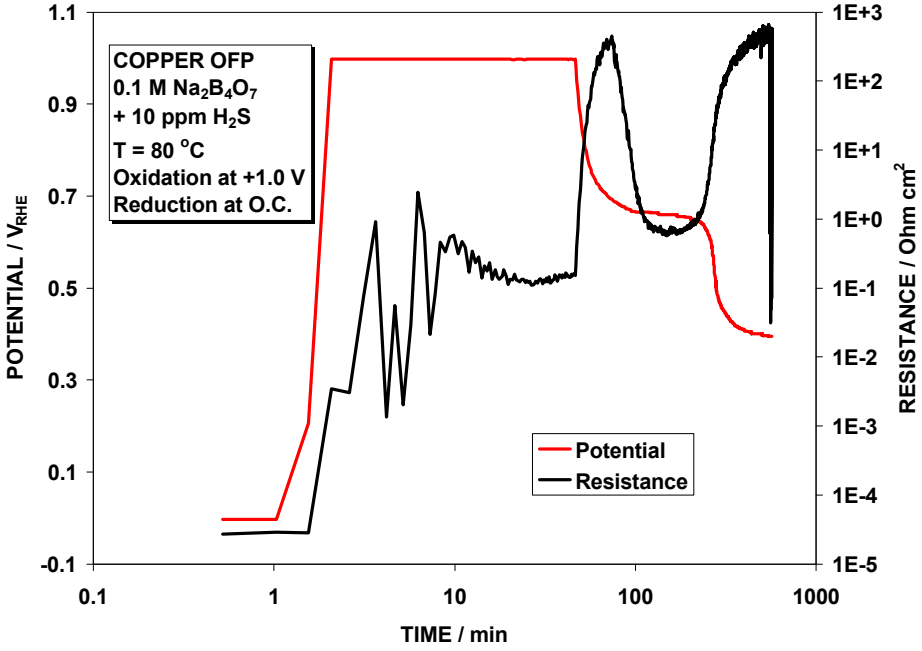

for time) during three successive stages - reduction at 0 V, oxidation at +1.0 V and reduction at open circuit.

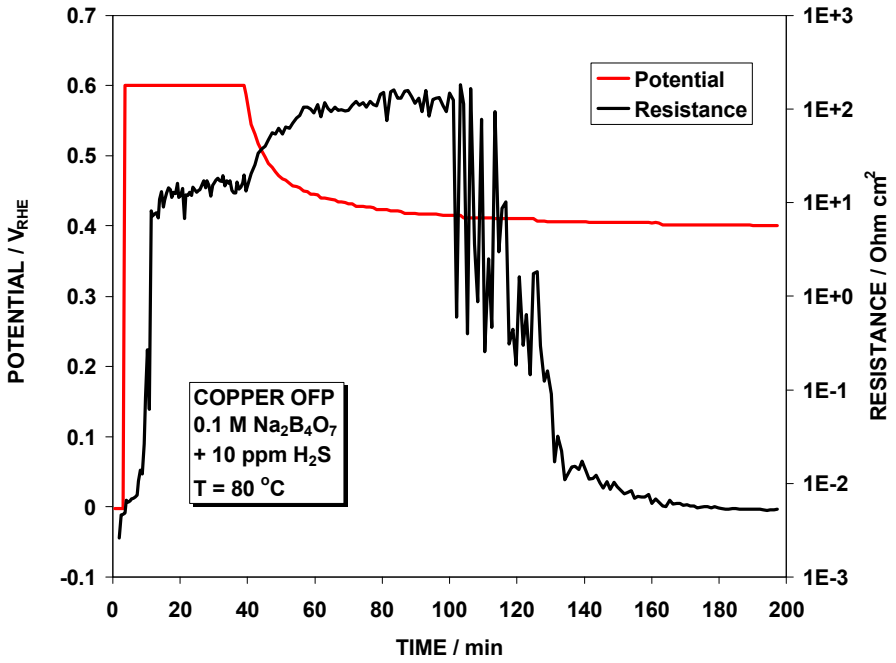

Figure 31. Resistance and potential as a function of time during three successive stages - reduction at 0 V, oxidation at +0.6 V and reduction at open circuit.

The open circuit potential and resistance as a function of time after potentiostatic oxidation at +1.0 V and at +0.6 V are shown in Figs 30 and 31, correspondingly (note that the time scale in Fig. 30 is logarithmic).

Figure 32 shows the open circuit potential and resistance as a function of time after a reduction at -0.45 V. The resistance increases to about $5*10^{-7}$ Ωcm^2 immediately after the polarisation is switched off and continues to increase slowly thereafter. The open circuit potential increases with a fast rate and approaches 0 V. This result together with the potentiodynamic result shown in Fig. 27 indicates that some adsorption of sulphide does occur on copper surface at these low potentials. The specific conductance of Cu_2S is $3.8*10^{-5}$ $\Omega^{-1}cm^{-1}$ [28]. From this value, assuming a thickness of 1 nm (about two atomic layers) the expected resistance of a Cu_2S surface film becomes $3*10^{-3}$ Ωcm^2. This is roughly four decades higher than what is experimentally measured, indicating again that a three dimensional film of Cu_2S is not formed.

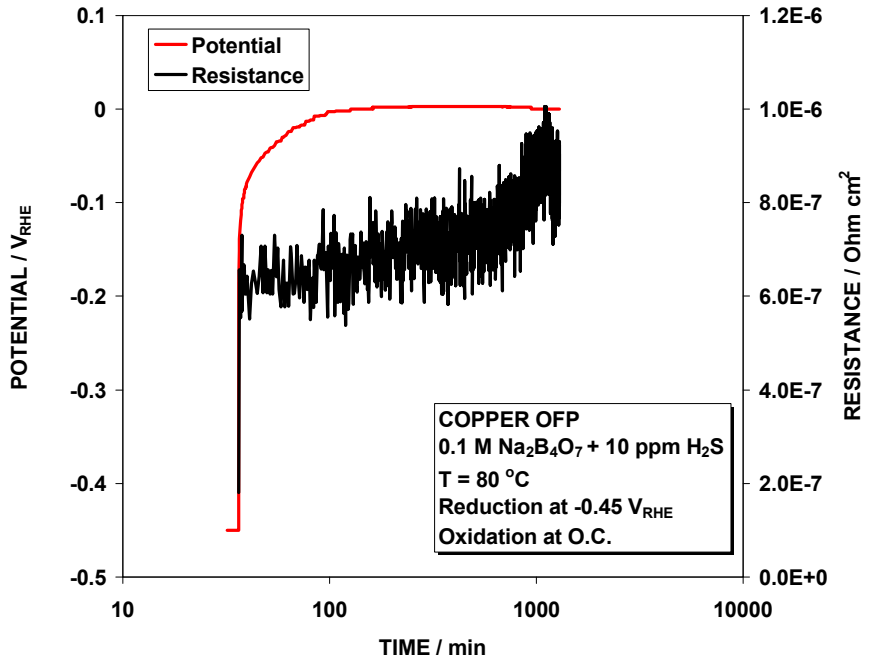

Figure 32. Resistance and potential as a function of time during two successive stages; reduction at -0.45 V and following oxidation at open circuit.

6.2.4 Impedance response of the films on copper in presence of sulphides

The impedance spectra shown in Fig. 33 are to a certain extent similar to those found for films grown in pure tetraborate solution. Two time constants were found for both the film grown at +0.6 V_{RHE} and for the film grown at +0.75 V_{RHE}. However, no transport impedance was detected in the presence of sulphide ions. This means that the ionic transport through the layer is no more the rate limiting step of the overall oxidation reaction. The equivalent circuit shown in Fig. 34 is also similar to that used for interpretation of the spectra measured for films grown in pure tetraborate solution, except for the absence of the Warburg element related to ionic transport through the film.

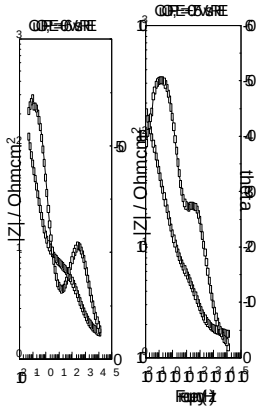

Figure 33. Impedance spectra for Cu OFP oxidised in 0.1 M $Na_2B_4O_7$ + 10 ppm H_2S (T = 80°C, p = 2 MPa) at E = 0.6 V_{RHE} (0.5 hrs) and E = 0.75 V_{RHE} (3 hrs).

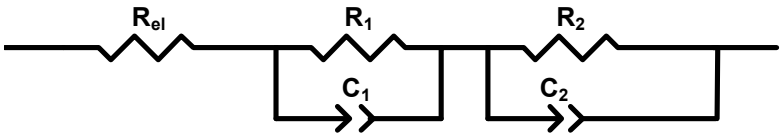

Figure 34. The equivalent circuit used in calculating the fitting parameters.

***Table VI**. Fitting parameters of the impedance spectra of Cu OFP oxidised at two different potentials in 0.1 M $Na_2B_4O_7$ + 10 ppm H_2S at T = 80 °C.*

0.6 V				**0.75 V**			
Electron conduction		Charge transfer		Electron conduction		Charge transfer	
R_1 Ωcm^2	C_1 μFcm^{-2}	R_2 Ωcm^2	C_2 μFcm^{-2}	R_1 Ωcm^2	C_1 μFcm^{-2}	R_2 Ωcm^2	C_2 μFcm^{-2}
6.4	107	460	10200	3.5	1000	336	6008

The fitting parameters, Table VI, found for Cu OFP oxidised at +0.6 V_{RHE} in the presence of 10 ppm of H_2S differ noticeably from those found in borax solution without H_2S. This indicates that the addition of 10 ppm of H_2S in the solution has a significant effect on the properties of the film formed on copper in the stability region of monovalent products. For the film formed at +0.6 V, the capacitance of the semiconducting part is much greater and correspondingly its resistance much smaller in the 10 ppm H_2S solution when compared to pure tetraborate solution. This points to the formation of a more defective layer in the presence of sulphide ions. This is in line with the absence of the transport limitations in this layer in solutions containing H_2S, as the transport of ions should be facilitated in a more defective layer. The rate of the charge transfer reaction, which is inversely proportional to R_2, is approximately the same both in

the absence and in the presence of sulphide ions. However, due to the absence of transport limitations in the film formed in the 10 ppm H_2S solution, the charge transfer becomes the rate limiting step of the oxidation. This leads to a higher corrosion rate of copper in the presence of sulphide ions.

Qualitatively, the differences between the fitting parameters found for Cu OFP after oxidising at +0.75 V_{RHE} in the presence and absence of sulphide ions were found to be similar as at +0.6 V. The charge transfer resistance R_2 increased markedly with time of oxidation at +0.75 V, see Table VII and Fig. 35. This was not the case in the pure tetraborate solutions, in which R_2 was found to be smaller and almost constant with time. Accordingly, sulphide ions seem to have some retarding effect on the charge transfer reaction.

***Table VII**. Fitting parameters for Cu OFP oxidised at +0.75 V_{RHE} in borax solution with 10 ppm of H_2S.*

Time / hours	R_1 / Ω cm^2	C_1 / μF cm^{-2}	R_2 / Ω cm^2	C_2 / μF cm^{-2}
3	3.5	1000	336	6010
6	3.4	1250	405	5900
9	3.6	1270	597	5800
12	3.8	1160	928	5590
15	4.0	1030	1060	5510
18	4.3	880	1310	5610
21	4.5	790	1430	5640

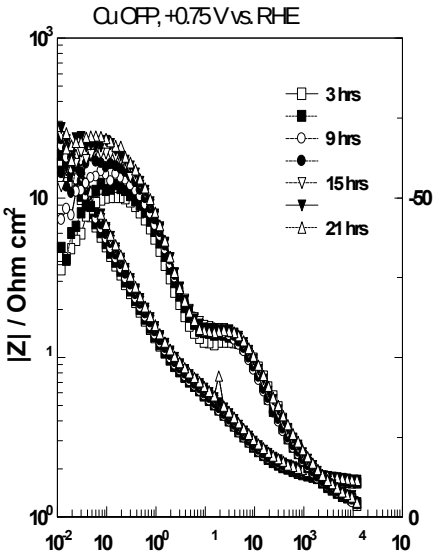

Figure 35. Time dependence of the impedance spectra of Cu OFP oxidised at +0.75 V_{RHE} in borax solution with 10 ppm H_2S.

6.3 Conclusions

The experimental data shown above indicate that 10 ppm of H_2S in 0.1 M $Na_2B_4O_7$ is not enough to promote the formation of three-dimensional copper sulphide films. The small indications of surface reactions and layers in the potential area where copper sulphides should form are likely to be caused by adsorption of sulphide on the surface, and not by the formation of a three dimensional sulphide film. These data are from short-term electrochemical experiments. Therefore, based on these data alone, one may not totally exclude the formation of copper sulphides during longer-term exposure.

The concentration of 10 ppm of H_2S in the solution was found to result in the formation of a much more defective film than in pure tetraborate solution. This leads to an increased ionic transport rate through the film. Thus in solutions containing sulphide ions the oxidation is no more limited by the ion transport but probably by the rate of the charge transfer step of film dissolution.

7. GENERAL CONCLUSIONS AND IMPLICATIONS FOR LOCALISED CORROSION

Localised corrosion, including pitting corrosion, stress corrosion cracking and environmentally enhanced creep is in different scenarios considered as a possible cause of failure of the copper shield. Surface films are presupposed to play an important role in localised corrosion. The aim of the present research program is to characterise the effect of different anions on the properties of surface films forming on copper in simulated disposal vault conditions and thereby to clarify the effect of the particular anions on the susceptibility of copper to the different forms of localised corrosion.

Based on the results some general conclusions can be made:

- The thickness of surface films (about 1 μm thick) forming on copper at 80 ^{o}C is roughly 100 times higher than that of films forming at room temperature. Therefore experimental work should be carried out at a temperature relevant to the final disposal vault conditions.
- Corrosion rate of copper is controlled by ionic transport through the outermost part of the oxide film and the charge transfer step of the film dissolution. The rate of the dissolution is affected by the presence of complexing agents in the electrolyte. Thus, the concentration and character of complexing agents in the water phase close to the copper canister surface deserves special attention. Known complexing agents for copper cations are e.g. nitrate and chloride ions.
- Chloride ions exert their detrimental effect exclusively on the surface film on copper in the stability region of divalent oxidation products, i.e. on the film forming on copper under oxidising conditions.

Further work should be directed to experiments performed under closely simulated disposal vault conditions, i.e. ground water of representative composition, and at the predicted temperature and pressure. The possibility of formation of soluble copper-chloride complexes at low potentials and very high chloride concentrations ($C_{Cl^-} > 1$ M) should be investigated experimentally. The effect of a longer term exposure (t > 10 days) of copper to a relevant sulphide concentration (i.e. $C_{H2S} < 10$ ppm) under relevant disposal vault conditions should be clarified. The experimental work should in general involve determination of surface film properties, creep tests in the environment and pitting corrosion tests. Possible cross-effects of several anions, e.g. sulphide, sulphate and chloride ions need to be verified. Modelling work should be carried out in order to combine the near-field transport phenomena with the release rate of copper ions from the canister surface.

8 REFERENCES

Mor, E.D.; Beccaria, A.M., Effects of temperature on the corrosion in different hydrostatic pressures, Werkstoffe und Korrosion v 30, 1979, p. 551-558.

2. Ahonen, L., Chemical stability of copper canisters in deep repository, Report YJT-95-19, Nuclear Waste Commission of Finnish Power Companies, December 1995.

Bertocci, U.; Turner, D.R.; Copper in Encyplopedia of electrochemistry of the , Marcel Dekker Inc., New York 1974, Vol 2, p. 383-497.

4. Leidheiser, H. Jr., The corrosion of copper, tin and their alloys, John Wiley and Sons, Inc. New York 1971, p. 71-125.

Van Muylder, J., Thermodynamics of Corrosion Comprehensive Treatise of

Press, New York and London 1981,Vol 4, p. 1-96.

6. Sequeira, C.A.C., Inorganic, physicochemical, and microbial aspects of copper corrosion:

7.

containers - reanalysis of a study of a bronze cannon, Applied Geochemistry v 10, 1995, p. 477-487.

Hallberg, R.O.; Ostlund, P.; Wadsten, T. Inferences from a corrosion study of a

3, 1988, p. 273-280.

9. Werme, L., Sellin, P. and Kjellbert, N., Copper canisters for nuclear high level waste disposal. Corrosion aspects. Technical Report SKB 92-26, Swedish Nuclear Fuel and

10.

canisters, Report YJT-94-13, Nuclear Waste Commission of Finnish Power Companies, August 1994.

Worgan, K.; Apted, M.; Sjoeblom, R., Performance analysis of copper canister

Management XVIII, Materials Research Society Symposium Proceedings v 353 1995, p. 695-702. Materials Research Society, Pittsburgh, PA, USA.

Grauer, R., The reducibility of sulphuric acid and sulphate in aqueous solutions, SKB

13.

Swedish Nuclear Power Inspectorate, July 1993.

14. SKI Report 95:6, International Seminar on Design and Manufacturing of Copper Canisters for Nuclear Waste. Swedish Nuclear Power Inspectorate, February 1995.

Stroes-Gascoyne, S.; West, J.M., Microbial considerations and studies in the fuel waste management program, Materials Research Society Symposium Proceedings v 353, n 1, 1995, p. 165-172. Materials Research Society,

16.

sulphate-reducing bacteria during microbiologically influenced corrosion of copper, Corrosion (Houston) v 47, n 9,Sep 1991, p. 674-677.

17. Hultquist, G., Hydrogen evolution in corrosion of copper in pure water, Corrosion Science v 26, 1986, p. 173-177.
18. Simpson, J.P.; Schenk, R., Hydrogen evolution from corrosion of pure copper, Corrosion Science v 27, n 12, 1987, p. 1365-1370.
19. Eriksen, T.E.; Ndalamba, P.; Grenthe, I. , On the corrosion of copper in pure water Corrosion Science v 29, n 10, Oct 1989, p. 1241-1250.
20. Ferreira, R. C. H., High-temperature diagrams for the systems, S-H_2O, Cu-S-H_2O, Fe-S-H_2O, in Leaching and reduction in hydrometallurgy, Ed. A.R. Burkin, London 1975, p. 67-83; Chen, C. H.; Aral, K., Computer-calculated Potential-pH Diagrams to 300°C. Volume 2: Handbook of diagrams. EPRI NP-3137. Palo Alto, CA, June 1983; Eh-pH diagrams for geochemistry, Brookins, Douglas G., Springer-Verlag, Berlin : New York. 1988, 176 s.
21. Mattson, E., Corrosion of Copper and Brass: Practical Experience in relation to Basic Data, British Corrosion Journal v 15, n 1, 1980, p. 6-13.
22. Perea, N.M.The Hyrkkölä native copper mineralization: A natural analogue for copper canisters, Scientific Basis for Nuclear Waste Management XX, Materials Research Society Symposium Proceedings v 465 1997. Materials Research Society, Pittsburgh, PA, USA. p. 1153-1160.
23. Ahonen, L., Chemical stability of copper canisters in deep repository, Report YJT-95-19, Nuclear Waste Commission of Finnish Power Companies, December 1995.
24. Horvath, J. and Hackl, L., Check of the potential/pH equilibrium diagrams of different metal-sulphur-water ternary systems by intermittent galvanostatic polarization method, Corrosion Science v 6, 1965, p. 525-538.
25. Marcus, P., Sulfur-Assisted Corrosion Mechanisms and the Role of Alloyed Elements, in Corrosion mechanisms in theory and practice edited by Marcus, P. and Oudar, J. Marcel Dekker Inc. New York 1995, p. 239-263.
26. Marcus, P.; Protopopoff, E., Potential- pH Diagrams for Adsorbed Species. Application to Sulphur Adsorbed on Iron at 25° and 300°C, Journal of the Electrochemical Society v 137, n 9, September 1990, p. 2709-2712; Marcus, P.; Protopopoff, E., Potential pH Diagrams for Sulphur and Oxygen Adsorbed on Nickel in Water at 25° and 300°C, Journal of the Electrochemical Society v 140, n 6, June 1993, p. 1571-1575; Marcus, P.; Protopopoff, E., Potential pH Diagrams for Sulphur and Oxygen Adsorbed on Chromium in Water, Journal of the Electrochemical Society v 143, n 5, May 1997, p. 1586-1590.
27. de Chialvo, M. R. Gennero; Arvia, A. J., Electrochemical behaviour of copper in alkaline solutions containing sodium sulphide, Journal of Applied Electrochemistry v 15, n 5, Sep. 1985, p. 685-696.
28. Khairy, E.M.; Darwish, N.A., Studies on copper semiconducting layer-electrolyte systems - I. Electrode potentials of copper and electrodeposited copper sulphide in S^{2-} and Cu^{2+} media, Corrosion Science v 13, 1973, p. 141-147.
29. Khairy, E.M.; Darwish, N.A., Studies on copper semiconducting layer-electrolyte systems - II. Galvanostatic anodic polarization of $Cu/Cu_2S/S^{2-}$ applying stationary and rectangular pulse tecniques, Corrosion Science v 13, 1973, p. 149-164.
30. Vasquez Moll, D.; de Chialvo, M.R.G.; Salvarezza, R.C.; Arvia, A.J., Corrosion and passivity of copper in solutions containing sodium sulphide. Analysis of potentiostatic current transients, Electrochimica Acta v 30, 1985, p. 1011-1016.

31. Scharifker, B.; Rugels, R.; Mozota, J., Electrocrystallisation of copper sulphide (Cu_2S) on copper, Electrochimica Acta v 29, n 2, 1984, p. 261-266.
32. Syrett, B., C., Accelerated Corrosion of Copper in Flowing Pure Water Contaminated with Oxygen and Sulfide, Corrosion (Houston) v 33, n 7, July 1977, p. 257-262.
33. Strehblow, H.H. ; Titze, B., The investigation of the passive behaviour of copper in weakly acid and alkaline solutions and the examination of the passive films be ESCA and ISS, Electrochimica Acta v 25, 1980, p. 839-850.
34. Lam, K.W., Ontario Hydro studies on copper corrosion under waste disposal conditions. Ed. D.W. Shoesmith, Whiteshell Nuclear Research Establishment. Proceedings of a workshop on corrosion of nuclear fuel waste containers. Jan 1990, p. 155-171.
35. Fontana, M., *Corrosion engineering,* 3rd edn., McGraw-Hill Inc., Singapore 1987, 556 pages.
36. King, P.; LeNeveu, D.M.; Jobe, D.J., Modelling the effects of evolving redox conditions on the corrosion of copper containers Scientific Basis for Nuclear Waste Management XVII, Materials Research Society Symposium Proceedings v 333, 1994, p 901-908. Materials Research Society, Pittsburgh, PA, USA.
37. Aaltonen, P., Hänninen, H., Klemetti, K. and Muttilainen, E., A literature study on corrosion of copper in disposal conditions of spent nuclear fuel (in Finnish), Report YJT-84-17, Nuclear Waste Commission of Finnish Power Companies, April 1984.
38. Thierry, D and Sand, W., Microbially Influenced Corrosion, in Corrosion mechanisms in theory and practice, edited by Marcus, P. and Oudar, J. Marcel Dekker Inc. New York 1995, p. 239-263.
39. Hermansson, H.-P., Some properties of copper and selected heavy metal sulphides, SKI Report 95:29, June 1995.
40. McNeil, M. B.; Little, B. J., Corrosion product and mechanims in long-term corrosion of copper, Scientific Basis for Nuclear Waste Management XIV Materials Research Society Symposium Proceedings v 212, 1991, p. 311-316. Publ by Materials Research Society, Pittsburgh, PA, USA.
41. Sjoeblom,R. ; Hermansson,H.P.; Amcoff,O. Chemical durability of copper canisters under crystalline bedrock repository conditions, Scientific Basis for Nuclear Waste Management XVIII, Materials Research Society Symposium Proceedings v 353, 1995, p. 687-694. Materials Research Society, Pittsburgh, PA, USA.
42. Edwards, M.; Meyer, T.; Rehring, J., Journal of American Water Works Association v 86, n 12, Dec 1994, p. 73-81; Edwards, Marc; Ferguson, John F.; Reiber, Steve H., Pitting corrosion of copper, Journal / American Water Works Association v 86, n 7, Jul 1994, p. 74-90; Edwards, M.; Rehring, J.; Meyer, T., Inorganic anions and copper pitting, Corrosion (Houston) v 50, n 5, May 1994, p. 366-372.
43. Duthil, J.-P.; Mankowski, G.; Giusti, A., Synergetic effect of chloride and sulphate on pitting corrosion of copper, Corrosion Science v 38, n 10, Oct 1996, p. 1839-1849.
44. Mankowski, G.; Duthil, J.P.; Giusti, A., Pit morphology on copper in chloride- and sulphate-containing solutions, Corrosion Science v 39, n 1, Jan 1997, p. 27-42.
45. Schmuki, P.; Boehni, H., Metastable pitting and semiconductive properties of passive films, Journal of the Electrochemical Society v 139, n 7, Jul 1992, p. 1908-1913.

46. Pourbaix, M. Atlas of Electrochemical Equilibria in Aqueous Solutions. p. 384-392, CEBELCOR, NACE International, Houston 1974.
47. Schöppel, H. R. and Gerischer, H., Die Kathodische Reduktion von Cu-I-oxid-Elektroden als Beispel fuer den Mechanismus der Reduktion eines Halbleiter-Kristalls. Ber. Bunsenges. Phys. Chem., v 75, 1971, p. 1237-1239.
48. Paatsch, W., Photoelectric measurements during corrosion and inhibition of copper in aqueous solutions, Ber. Bunsenges. Phys. Chem., v 81, 1977, p. 645-648.
49. Hardee, K. L. and Bard, A. J., Semiconductor electrodes, X. photoelectrochemical behaviour of several polycrystalline metal oxide electrodes in aqueous solutions, J. Electrochem. Soc., v 124, 1977, p. 216-224.
50. Yamashita, M., Omura, K. and Hirayama, D., Passivating behaviour of copper anodes and its illumination effects in alkaline solutions, Surface Science, v 96, 1980, p. 443-460.
51. Abrantes, L. M., Castillo, L. M., Norman, C. and Peter, L. M., A photoelectrochemical study of the anodic oxidation of copper in alkaline solutions, J. Electroanal. Chem., v 163, 1984, p. 209-221.
52. Burleigh, T.D., Anodic photocurrents and corrosion currents on passive and active-passive metals, Corrosion, v 45, 1989, p. 464.
53. Collisi, U. and Strehblow, H.-H., The formation of Cu_2O layers on cu and their electrochemical and photoelectrochemical properties, J. Electroanal. Chem., v 284, 1990, p. 385-401.
54. Sathiyanarayanan, S., Manoharan, Sp., Rajagopal, G. and Balakrishnan, K., Characterisation of passive films on copper, British Corrosion Journal, v 27, 1992, p. 72-74.
55. Trabanelli, G., Zucchi, F. and Brunoro, G., Photoelectrochemical measurements in the study of surface layers in metal corrosion, inhibition and passivation phenomena, Thin Solid Films, v 13, 1972, p. 131.
56. Di Quarto, F., Piazza, S. and Sunseri, C., Photoelectrochemical study of the corrosion product layers on copper in weakly acidic solutions, Electrochimica Acta, v 30, 1985, p. 315-324.
57. Modestov, A. D., Zhou, G.-D., Ge, H.-H. and Loo, B. H., A study by voltammetry and the photocurrent response method of copper electrode behaviour in acidic and alkaline solution containing chlorides, Journal of Electroanalytical Chemistry v 380, 1995, p. 63-68.